1999-09

Southern Hemisphere Application of the Systematic Approach to Tropical Cyclone Track Forecasting. Part III : updated environmental structure characteristics

Reader, Grahame; Boothe, Mark A.; Elsberry, Russell L.; Carr, Lester E. III

Monterey, California. Naval Postgraduate School Department of Meteorology

NPS-MR-99-004

NAVAL POSTGRADUATE SCHOOL
Monterey, California

Southern Hemisphere Application of the Systematic Approach to Tropical Cyclone Track Forecasting
Part III:
Updated Environmental Structure Characteristics

Grahame Reader, Mark A. Boothe, Russell L. Elsberry and Lester E. Carr, III

September 1999

Prepared for: SPAWARSYSCOM
Code PMW 185, San Diego, CA 92110-3127

Naval Postgraduate School
Monterey, California 93943-5000

Rear Admiral Robert C. Chaplin
Superintendent

Richard S. Elster
Provost

This report was prepared for the Space and Naval Warfare Command (PMW 185) under Program Element 0604 207N entitled: "Systematic Approach Tropical Cyclone Forecast Techniques." The technique is intended for application at the Joint Typhoon Warning Center (JTWC) at the Naval Pacific Meteorology and Oceanography Center (NPMOC), Pearl Harbor, Hawaii.

This report was prepared by:

Grahame Reader by RLE
Grahame Reader
Bureau of Meteorology,
Perth, Australia

Mark Boothe
Mark A. Boothe
Meteorologist

Lester E. Carr III by RLE
Lester E. Carr, III
Research Associate Professor of Meteorology

Russell L. Elsberry
Russell L. Elsberry
Professor of Meteorology

Reviewed by:

Kenneth D Davis
For Carlyle H. Wash, Chairman
Department of Meteorology

Released by:

D. W. Netzer
David W. Netzer
Dean of Research

REPORT DOCUMENTATION PAGE

Form approved

OMB No 0704-0188

1. AGENCY USE ONLY	2. REPORT DATE	3. REPORT TYPE AND DATES COVERED
	September 1999	Interim 10/98 - 09/99

4. TITLE AND SUBTITLE
Southern Hemisphere Application of the Systematic Approach to Tropical Cyclone Track Forecasting: Part III. Updated Environmental Structure Characteristics

5. FUNDING
N0003900WRDF203

6. AUTHOR(S)
Grahame Reader, Mark A. Boothe, Russell L. Elsberry, and Lester E. Carr, III

7. PERFORMING ORGANIZATION NAME AND ADDRESS
Naval Postgraduate School
Department of Meteorology
589 Dyer Rd., Room 254
Monterey, CA 93943-5114

8. PERFORMING ORGANIZATION REPORT NUMBER

9. SPONSORING/MONITORING AGENCY NAME AND ADDRESS
Space and Naval Warfare Systems Command
PMW 185, San Diego, CA 92110-3127

10. SPONSORING/MONITORING AGENCY REPORT NUMBER

11. SUPPLEMENTARY NOTES
The views expressed in this report are those of the authors and do not reflect the official policy or position of the Department of Defense.

12a. DISTRIBUTION/AVAILABILITY STATEMENT
Approved for Public Release; Distribution Unlimited

12b. DISTRIBUTION CODE

13. ABSTRACT The Meteorological knowledge base of the Systematic Approach to tropical cyclone track forecasting in the Southern Hemisphere has been updated to reflect a more global terminology. Examples of these new environment structures in operational (NOGAPS) analyses and tracks are given. Perhaps the most important conclusion is that all cases in the 1990-91 through 1998-1999 seasons could be classified into one of these 14 synoptic pattern/region combinations. The nine-year "climatology" of the occurrences of each of the 14 combinations is given for the South Indian and Pacific Oceans separately, and the characteristic tracks in each of these 14 combinations are provided. Some new transitional mechanisms between these combinations have also been defined. The importance of these transitions from one pattern/region combinations to another is that the TC track then also changes. The frequency of recurring (greater than three) transitions in this nine-year sample is summarized. Because the TC is at any time in only one pattern/region combination, the concern of the forecaster is on the possible transitions from that pattern/region. To assist the forecaster, the percentages of these transitions from each pattern/region combination are also summarized. Some of these transitions are clearly more favored than others, which is useful guidance to the forecaster.

14. SUBJECT TERMS
Tropical cyclone track forecasting; Tropical cyclone motion

15. NUMBER OF PAGES
73

16. PRICE CODE

17. SECURITY CLASSIFICATION OF REPORT	18. SECURITY CLASSIFICATION OF THIS PAGE	19. SECURITY CLASSIFICATION OF ABSTRACT	20. LIMITATION OF ABSTRACT
Unclassified	Unclassified	Unclassified	

TABLE OF CONTENTS

LIST OF FIGURES

LIST OF TABLES

ACKNOWLEDGMENTS

This research has been sponsored by the Space and Naval Warfare Systems Command. The original concept of the Systematic Approach to Tropical Cyclone Track Forecasting was developed over several years with funding from the Office of Naval Research Marine Meteorology Program under the management of Robert F. Abbey, Jr. This two month visit by Grahame Reader is the third collaboration with the Australian Bureau of Meteorology in Perth. The Bureau of Meteorology funded the salary and this SPAWAR contract paid the travel and per diem to facilitate this exchange. Best-track tropical cyclone records were provided by the Joint Typhoon Warning Center, Pearl Harbor, Hawaii, and NOGAPS analyses were provided by the Fleet Numerical Meteorology and Oceanography Center, Monterey, California. Mrs. Penny Jones expertly typed the manuscript.

1. INTRODUCTION

a. *Systematic Approach framework*

The basic concepts of a Systematic and Integrated Approach to Tropical Cyclone (TC) Track Forecasting (hereafter the Systematic Approach) were introduced by Carr and Elsberry (1994) for the western North Pacific region. The central thesis of the Systematic Approach is that the forecaster can formulate track forecasts that improve on the accuracy and/ or consistency of the dynamical or other objective guidance if he/she is equipped with: (*i*) a Meteorological knowledge base of dynamically sound conceptual models that classify various TC-environment situations: (*ii*) a knowledge base of recurring TC track forecast errors attributed to various combinations of TC structure and environment structure, and the anticipated changes; and (*iii*) an implementing methodology or strategy for applying these two knowledge bases to particular TC forecast situations.

The basic components of the Meteorological knowledge base in the Systematic Approach are given in Fig. 1. Environment structure is defined in terms of synoptic patterns and synoptic regions. Synoptic patterns are classifications of the large-scale environment based on the existence and orientation of circulations such as cyclones and anticyclones. Synoptic regions are smaller regions within the synoptic patterns where certain characteristic directions of environmental steering of the TC may be expected. The TC structure is described in terms of traditional intensity categories and distinguish between midget, small, average, and large sizes. The motivation for the size grouping, and proposed strategy for determining operationally the size, is given by Carr and Elsberry (1997).

A key element of the Systematic Approach is to recognize transitional mechanisms (lower portion of Fig. 1) that will lead to a transition in the environment structure. Because each

such synoptic pattern/region transition is associated with a TC track change, it is important that the forecaster be equipped to recognize that a transition is (or will be) occurring. Equipping forecasters to recognize these changes in environment structure is a major goal of the Systematic Approach.

Carr *et al.* (1995) prepared a climatology of 12-h TC and environment structure characterizations for all TCs in the western North Pacific during 1989-1993, and this lead to a refinement of the Systematic Approach. This climatology has subsequently been extended through the 1997 TC season for the western North Pacific. A similar climatology of the environmental structure has been prepared in the eastern and central North Pacific (White 1995, Boothe 1997), and also for the Atlantic (Kent 1995, Boothe *et al.* 1999). Bannister *et al.* (1997, 1998) examined the possible adaptation of the Systematic Approach Meteorological knowledge base to all Southern Hemisphere TCs during the 1990-91 through 1997-98 seasons.

Although the synoptic patterns and synoptic regions that make up the environment structure vary slightly in the TC basins examined thus far, the important conclusion is that all TC scenarios have been able to be classified with only a small set of conceptual models. Furthermore, the basic Systematic Approach concepts of associating characteristic TC tracks with specific synoptic environment circulations, and identifying TC structure characteristics that may lead to an environment structure change, have been demonstrated to be valid. Making allowance that the specific transformation mechanisms do vary among the TC basins examined thus far, a (retrospective) explanation for all significant track changes has been possible in terms of only a small set of transitional mechanisms.

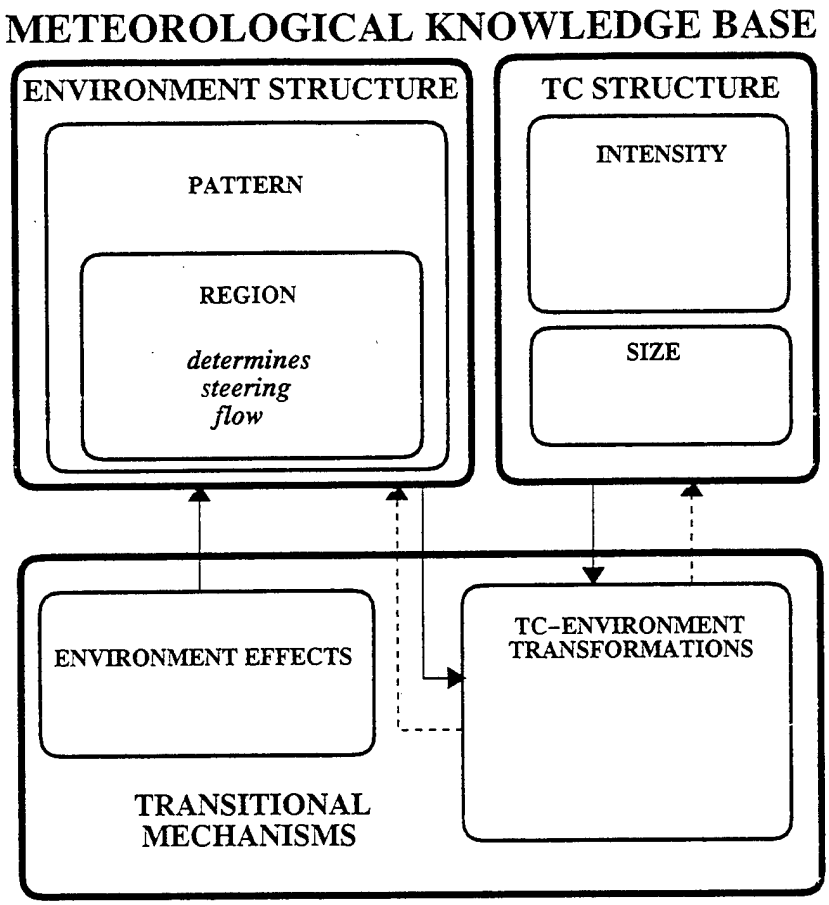

Fig. 1. General framework of the Meteorological knowledge base of the Systematic Approach with the Environment structure and the TC structure that describe the present situation and the transitional mechanisms of environment effects and TC-environment transformations that are operating to change the track.

The Joint Typhoon Warning Center (JTWC), Hawaii, forecasters have utilized the environment structure aspect of the Systematic Approach for several seasons. The second knowledge base of recurring track forecast errors has recently been developed for western North Pacific TCs (Carr and Elsberry 1999), and preliminary versions have been introduced to JTWC forecasters. The third aspect of an implementing methodology is still in development.

b. Objectives

The primary objectives of this study have been to redefine and extend the Southern Hemisphere adaptation of the Systematic Approach Meteorological knowledge base. That is, this study addresses the first step in the Systematic Approach described in section 1.a above, and

sets the stage for developing a Model Traits knowledge base and an implementing methodology. New understandings have been gained in the applications of the Systematic Approach to the eastern/central North Pacific (Boothe 1997), the Southern Hemisphere (Bannister *et al.* 1997, 1998), and recently for the Atlantic (Boothe *et al.* 1999). These studies have led to new terminology for the environment structure and transitional mechanisms that are believed to have global applicability.

In section 2, the Southern Hemisphere TC environment structure classifications by Bannister *et al.* (1997, 1998) are updated for the new terminology given in Fig. 2. The goal is to identify synoptic patterns and synoptic regions that the Southern Hemisphere forecaster may use to develop a "storyline" that explains the present and recent past TC motion, i.e., a physically based environment structure description of the circulations that are determining the present track. As Carr and Elsberry (1999) have demonstrated, it is the ***improper representation*** of these circulations in the numerical models that often leads to large track forecast errors. Thus, it is important to identify these circulations in the model initial conditions to continue consistently the storyline into the forecast period.

In section 3, the new environment structure and transitional mechanism terminology is applied to classify the 1998-99 TCs in the Southern Hemisphere. Thus, a new "climatology" of synoptic patterns and regions is prepared by adding the 1998-99 data set to the updated data base of Bannister *et al.* (1997, 1998). Characteristic track segments associated with each synoptic pattern/region combination will be presented. As various physical mechanisms have been identified that lead to changes in the TC track, some new conceptual models will be introduced that describe the environment structure changes leading to the track changes. Case studies that illustrate the sequence of environment structure changes in operational analyses will be

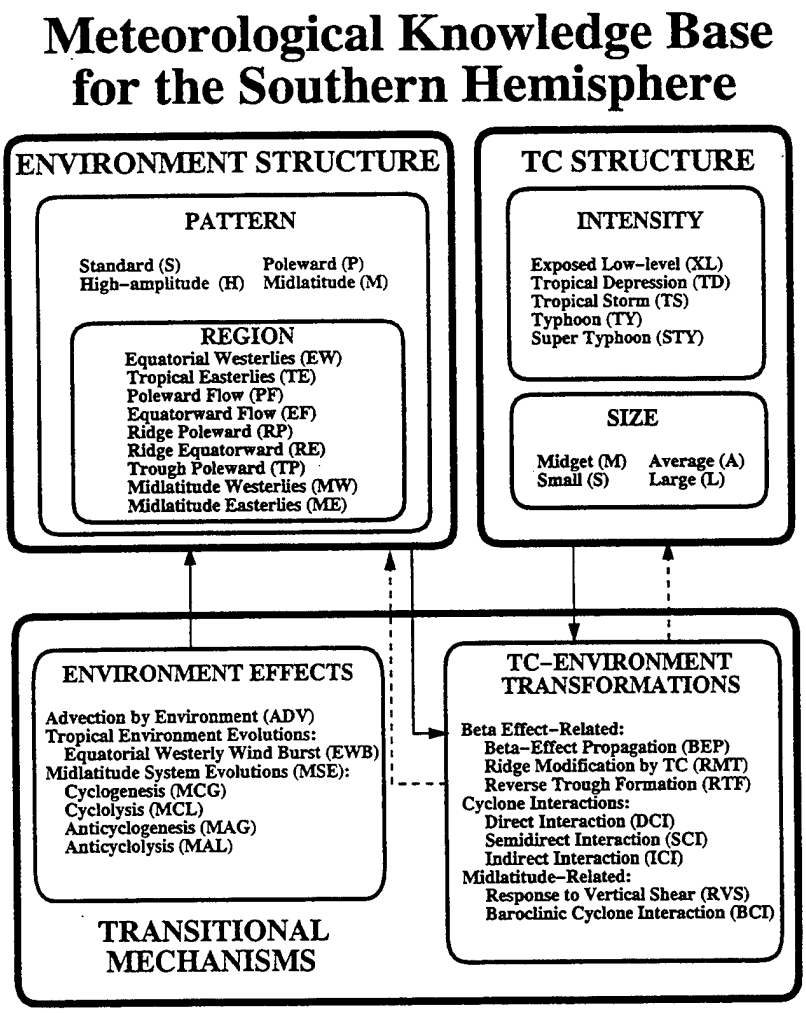

Fig. 2 Meteorological knowledge base as in Fig. 1, except specifically for application of the Systematic Approach to the Southern Hemisphere TCs as modified in this report from that by Bannister *et al.* (1998).

presented. An updated "climatology" of environment structure changes has been prepared as a basis for assessing how often specific transitions from one synoptic pattern/region combination to another combination occur. Given knowledge of the synoptic pattern/region, only certain transitions to other pattern/region combinations have been observed. It is useful background for the forecaster to know how common or how rare an anticipated synoptic pattern/region transition (and thus an associated track change) is.

In summary, the updated and refined Meteorological knowledge base described in sections 2-3 will assist the forecaster in the essential first step in forecasting, which is to do a

careful analysis of the synoptic situation for the purpose of understanding what circulations and physical mechanisms are determining the present TC track. Knowing well the present synoptic situation leads to the second step in forecasting, which is utilization of the available guidance (dynamic models, statistical and empirical techniques) to predict the future track as accurately as possible.

2. APPLICATION OF NEW TERMINOLOGY TO EXISTING DATA BASE

Bannister *et al.* (1997, 1998) adapted the Systematic Approach Meteorological knowledge base to TCs during eight seasons (1990-91 through 1997-98), which included 145 (90) TCs in the South Indian (Pacific) region. A total of 2357 TC-environment structure classifications were described by only the four synoptic patterns and 11 synoptic regions depicted in Fig. 3. The re-labeling of the synoptic pattern/region combinations for the TCs in this eight-year data base will be described in this section.

As indicated in section 1.b, new terminology has been introduced that is intended to be applicable throughout the global TC regions. The proposed terminology for classifying Southern Hemisphere TC synoptic pattern and regions is illustrated in Fig. 4. Each of the changes from the terminology in Fig. 3 will be described in the following subsections. It is emphasized that the idealized schematics in Figs. 3 and 4 should be regarded as templates to be adjusted to fit variability in the actual circulation structures.

One basic interpretation of these TC-environment structure classifications at the Bureau of Meteorology Office in Perth is whether today's synoptic situation is basically zonally oriented versus meridionally oriented. In Fig. 4, the Standard (S) and Midlatitude (M) patterns may be interpreted as zonally oriented, even though one variation of each of these patterns is for more circular-shaped subtropical anticyclone circulations than in these schematics. Whereas the Poleward (P) pattern has meridional flow, this is mainly within the tropics (equatorward of the subtropical ridge) and accounts for a steering flow that moves the TC out of the deep tropics. Each of the S, M, and P patterns has counterparts in every other TC basin studied (only the North Indian basin has not been studied). That is, these three basic synoptic patterns are found throughout (most of) the globe.

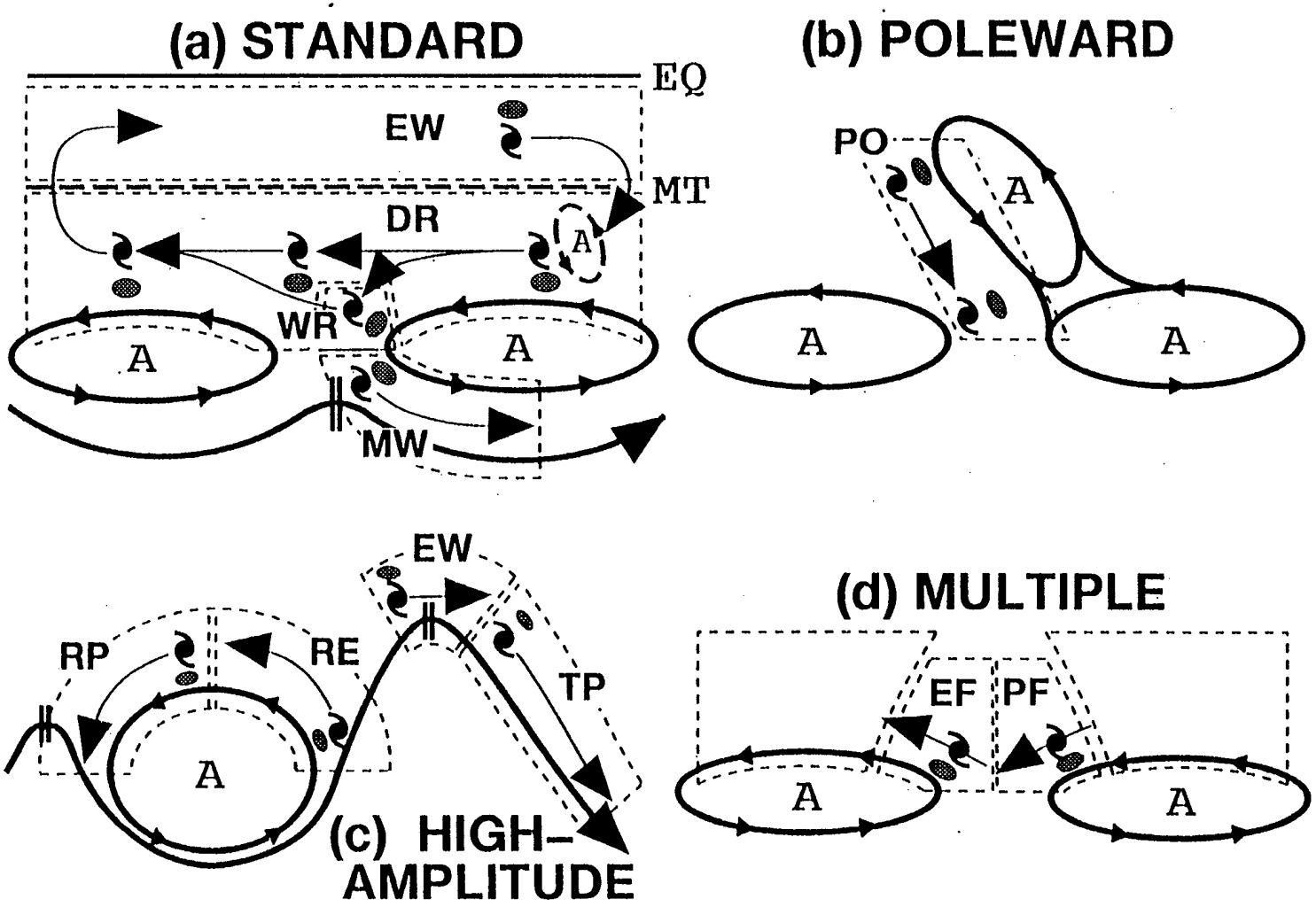

Fig. 3 Summary of the four synoptic patterns and associated synoptic regions for the Systematic Approach Meteorological knowledge base in the Southern Hemisphere (Bannister *et al.* 1997, 1998). The symbols EQ, MT, and A are for Equator, Monsoon Trough, and Anticyclone.

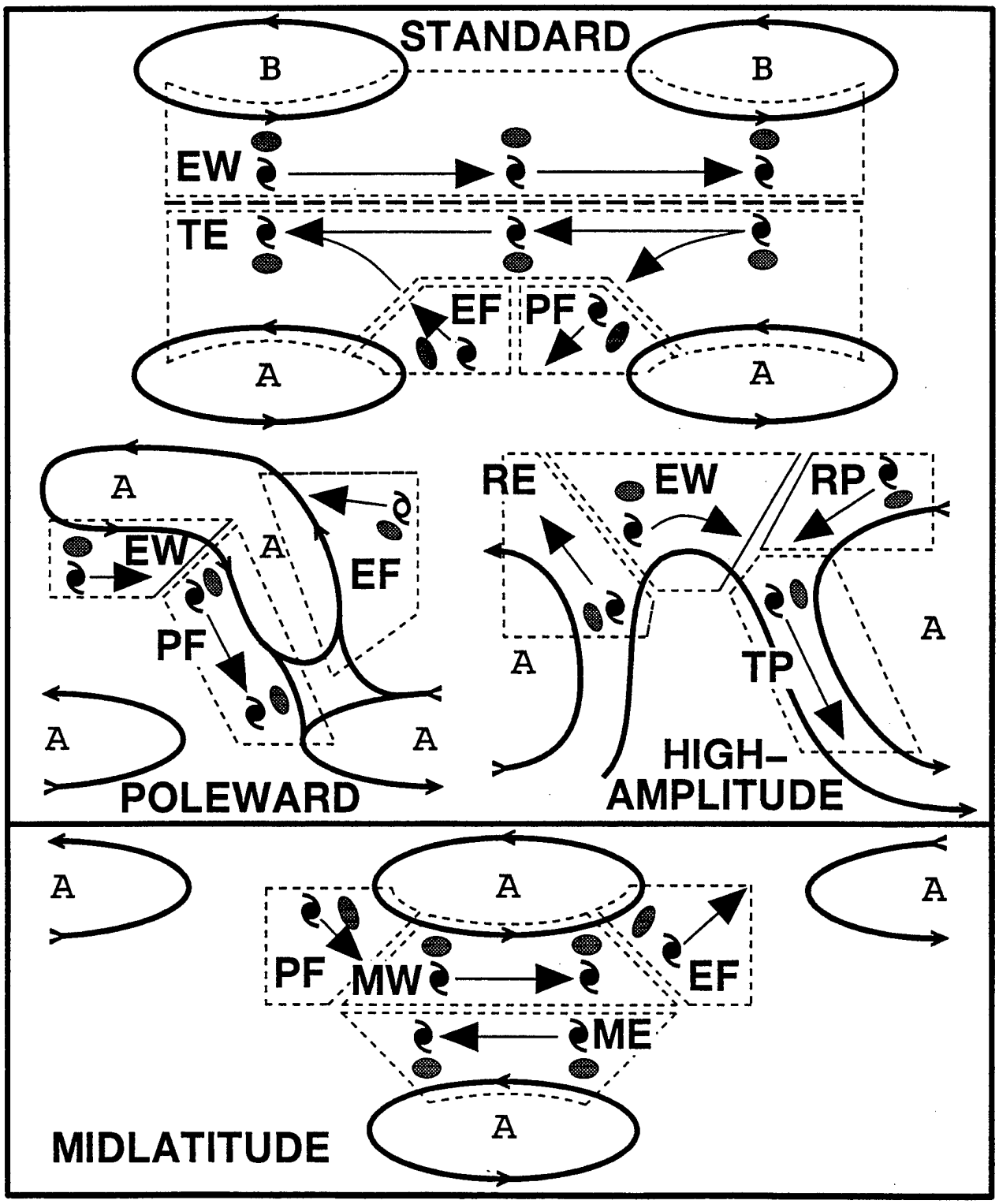

Fig. 4. New conceptual models and synoptic pattern and region terminology proposed for the Southern Hemisphere.

As Bannister *et al.* (1997, 1998) emphasize, the unique synoptic pattern for Southern Hemisphere TCs is the High-amplitude (H) pattern in which midlatitude troughs and ridges may penetrate almost to the Equator. Thus, these troughs and ridges are the "ultimate" in meridionally-oriented flow such that the forecaster should pay particular attention. In the H/TP pattern/region, the midlatitude circulation dominates over the subtropical anticyclone as the primary steering flow for the TC.

One principle in the new terminology has been to label the synoptic regions with a directionality of the TC steering flow. For example, the Equatorial Westerlies (EW), Tropical Easterlies (TE), Midlatitude Westerlies (MW), and Midlatitude Easterlies (ME) synoptic regions in Fig. 4 clearly imply the direction of the environmental steering for the TC. Similarly, the Equatorward Flow (EF), and Poleward Flow (PF) synoptic regions indicate a steering flow directionality. This naming principle has been somewhat modified for the unique H pattern with its high amplitude troughs and ridges that determine the TC-environment structure. In this pattern, the synoptic regions have an equatorward or poleward directionality implied, but the emphasis is whether it is the Trough (TP) or the adjacent Ridge (RE or RP) that is the primary determinant of the steering flow of the TC. Whereas the RE and RP regions of the H pattern have similarities with the EF and PF regions of the S pattern, it was decided to keep the special terminology of Bannister *et al.* (1997, 1998) for the H pattern.

The Systematic Approach environment structure conceptual models are applied with real-time U. S. Navy Operational Global Atmospheric Prediction System (NOGAPS) analyses from the Fleet Numerical Meteorology and Oceanography Center (FNMOC), Monterey, California. Beginning in June 1990, synthetic observations have been included in the NOGAPS analyses to improve the TC location and structure representation. These synthetic observations for Southern

Hemisphere TCs have been based on the Joint Typhoon Warning Center (JTWC) warning messages. Since October 1994, the synthetic observations have included an adjustment to make the average flow in the region of the TC agree with the recent 12-h motion of the storm as contained in the JTWC warnings. The synthetic observations, any rawinsondes or other observations, and a 6-h NOGAPS forecast are blended in the data assimilation system to provide the initial conditions for the global model forecast. Although the 500-mb analyses are typically used to characterize the synoptic pattern/region that determines the steering flow, analyses at 700 mb or lower may be used when the TC is weak or vertical wind shear has affected the upper-tropospheric structure.

One helpful feature in classifying the environment structure (synoptic pattern/region) is the position of the isotach maximum relative to the TC position, which is indicated in Figs. 3 and 4 as a shaded ellipse. Given that the TC vortex is embedded in a steering current, the winds will be higher (lower) on the left (right) side looking in the direction of motion (Southern Hemisphere). Because 13 synthetic TC observations are inserted in the NOGAPS analysis whenever the JTWC detects a tropical depression or stronger TC, and (since October 1994) the average of these 13 observations is adjusted to equal the past 12-h storm motion, the position of the isotach maximum is a proxy for the steering flow. This assumes that enough observations exist over the Southern Hemisphere to define the environmental flow, which is not always the case. As an example, the isotach maximum is expected to be on the southern side of a TC that is translating westward in the Tropical Easterlies (TE) of the Standard pattern (Fig. 4), and be on the southeastern side as the TC moves southwestward in the Poleward Flow (PF) region of the Standard pattern. If the TC fails to recurve and begins to move north of west in the Equatorward Flow (EF) region of the Standard pattern, the isotach maximum will suddenly shift to the west-

southwest of the TC. However, if the TC recurves through the subtropical anticyclone axis into the PF region of the Midlatitude pattern, the isotach maximum will be on the northeast side, and then on the northern side as the TC translates eastward in the Midlatitude Westerlies (MW) region of the Midlatitude pattern.

a. Changes in the Standard (S) pattern

Only a small change has been made in the S/Equatorial Westerlies (EW) pattern/region in Fig. 3 in which the TC is moving eastward on the equatorward side of the monsoon trough. The new schematic in Fig. 4 includes Buffer (B) cells that are counter-clockwise circulations that may straddle the Equator, and thus may not be unambiguously defined as anticyclones or cyclones. Whereas the TC may have formed in the EW region, it may also move into this region as a result of a transitional mechanism. Bannister *et al.* (1998, their Fig. 10) described a conceptual model of an Equatorial Westerly wind Burst (EWB) transitional mechanism (see list in Fig. 2 bottom). Approach of an Equatorial Westerlies wind burst on the equatorward side will change the westward steering flow of a TC in the S/Tropical Easterlies (TE) pattern/region to an eastward steering flow in the S/EW pattern/region (Note the new S/TE designator will be used versus the S/Dominant Ridge (DR) designator in their Fig. 10). Bannister *et al.* (1998) provide three examples of the EWWB transitional mechanism.

As indicated above, the S/TE designation for TCs moving westward in the easterly trade wind flow is the new terminology that is based on directionality of the steering flow in which the TC is embedded. It replaces the old S/DR terminology that was related to the strength of a circulation feature that was establishing that steering flow.

Similarly, the prior S/Weakened Ridge (WR), which again was related to the strength of a circulation feature, is replaced by the S/Poleward Flow (PF) pattern/region. The S/WR definition

included a deceleration of the TC translation speed as the TC moved into the col region between two subtropical anticyclones, which is the common experience in the western North Pacific region. In the more directional-based S/PF pattern/region on the northwestern flank of the eastern subtropical anticyclone cell, the TC translation speed may not slow if the western anticyclone is weak or displaced westward from the TC. Whereas the WR region was also assumed to be a small col area, a TC in the S/PF pattern/region may have a relatively long track compared to the prior S/WR tracks.

1. New S/EF pattern/region. A more major change in the new S pattern (Fig. 4) is the introduction of the Equatorward Flow (EF) region on the northeastern flank of the western subtropical anticyclone cell. One of the reasons for introducing this EF region is to account for the Semi-direct TC Interaction (STI) transitional mechanism defined by Carr and Elsberry (1994) and Carr *et al.* (1997). However, the conditions for this transitional mechanism (e.g., two TCs in an east-west orientation within 10° latitude of the subtropical anticyclone axis) were identical to the old Multiple (M) TC pattern (see Fig. 3d). Thus, the somewhat redundant Multiple TC synoptic pattern could be eliminated by the inclusion of the EF region in the S pattern, if it is understood that two TCs are occurring simultaneously in the EF and PF regions with the spatial orientation shown in Fig. 4. Rather than the STI transitional mechanism, this mechanism has now been generalized to include the possibility that the second TC is a cyclone (perhaps a tropical or monsoon depression, a downward extension of a Tropical Upper Tropospheric Trough (TUTT) cell, or a midlatitude cyclone). That is, the Semi-direct Cyclone Interaction (SCI) transitional mechanism in Fig. 2 (bottom right) has two variants. In the SCIW (Fig. 5a), the western TC in the S/EF pattern/region has a cyclone (which may be a TC) to the east. The equatorward steering flow across the western TC is attributed to the pressure gradient between

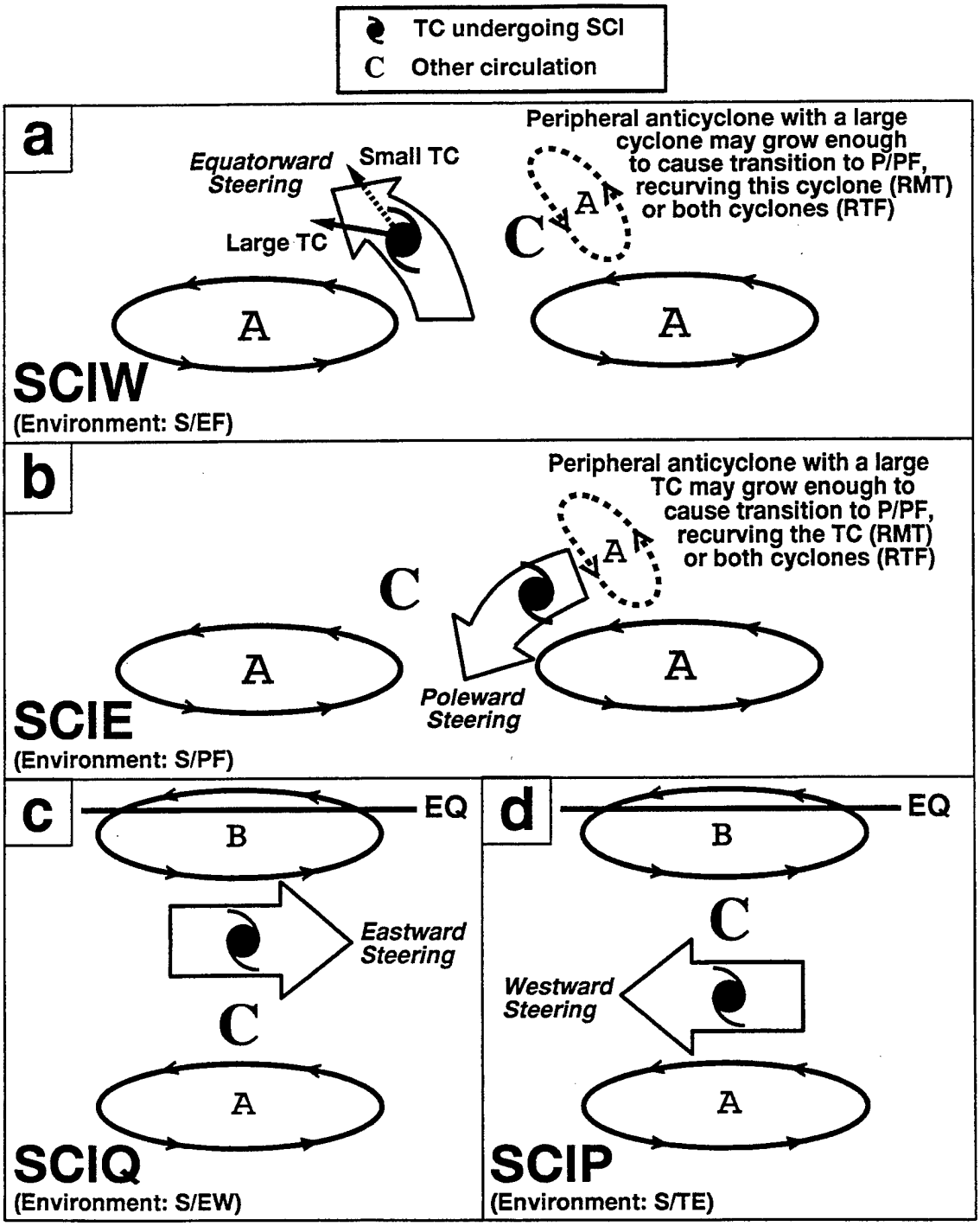

Fig. 5 Conceptual models of the Semi-direct Cyclone Interaction (SCI) transitional mechanism causing track deflections on the (a) western TC (SCIW) or (b) eastern TC (SCIE) owing to the steering flows (large open arrows) established by pressure gradients between adjacent high pressure in the subtropical anticyclone and the low pressure in the eastern (a) or western (b) cyclone. See Carr *et al.* (1997) for further depiction if two TCs are involved. In panels (c) and (d), the SCI on an equatorward TC (SCIQ) or a poleward TC (SCIP) aligned meridionally is illustrated following Bannister *et al.* (1998).

this eastern cyclone (low pressure) and the western subtropical anticyclone (high pressure). In the SCIE (Fig. 5b), the eastern TC in the S/PF pattern/region has a cyclone (which may be a TC) to the west. The poleward steering flow across the eastern TC is attributed to the pressure gradient between this western cyclone (low pressure) and the eastern subtropical anticyclone (high pressure). If both SCIW and SCIE are occurring simultaneously, the equatorward (poleward) deflections of the western (eastern) TC tend to terminate quickly the spatial orientation of the low and high pressures necessary for establishing these steering flows across the TCs, and thus end the SCI.

Bannister *et al.* (1998) also introduce a Semi-direct TC Interaction Equatorward (STIQ) and Poleward (STIP) conceptual model (their Fig. 18) and give examples. Even though all of the examples thus far of this transitional mechanism have involved two TCs, this mechanism will also be generalized to SCIQ or SCIP. As it is conceivable that the second cyclone could be a monsoon depression, the more general designator may be appropriate.

The second TC motion scenario implied by the new EF region in the S pattern (Fig. 4) is a single TC moving from the PF region to the EF region. Such a track change can lead to very large forecast errors if the TC is erroneously predicted to recurve around the eastern subtropical anticyclone and accelerate into the midlatitude westerlies. Thus, this "stairstep" track of westward motion in the S/TE, poleward in the S/PF, and then westward again in the S/EF pattern/region is a critical forecast scenario.

2. TC Melanie/Bellamine case study. Such a track for TC Melanie/Bellamine is shown in Fig. 6. At 12 UTC 30 October 1996, this TC is moving toward the south-southwest. At 0000 UTC 31 October, the TC motion has abruptly changed toward the northwest. Between

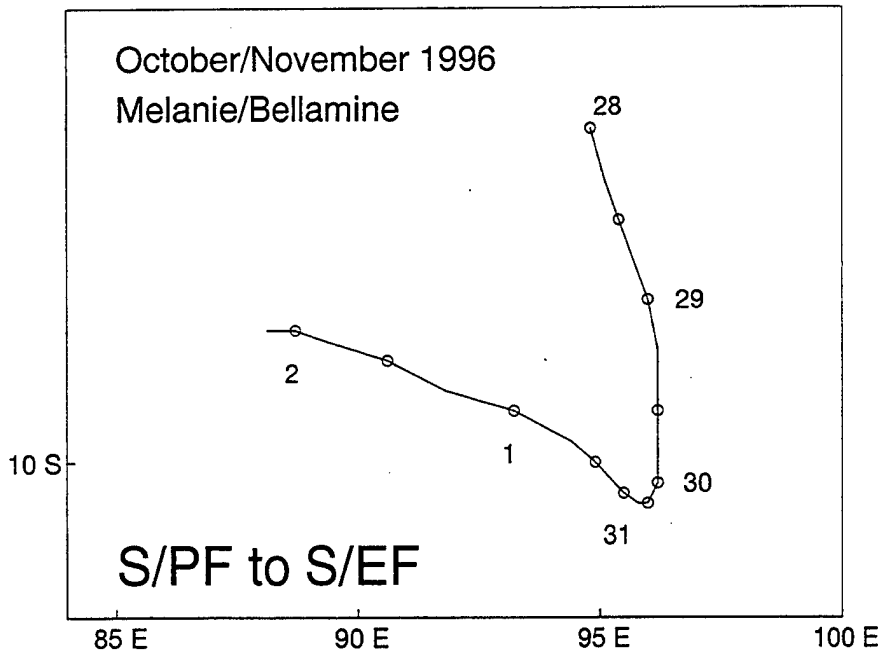

Fig. 6 Best track of TC Melanie/Bellamine during 0000 UTC 28 October 1996 to 0000 UTC 2 November. TC positions are indicated each 12 h (circles) with the date (large numeral) adjacent to the 0000 UTC position.

0000 UTC and 1200 UTC 1 November, TC Melanie/Bellamine accelerates toward the west-northwest and is moving at 13 kt by 1200 UTC. Clearly, this track change would have led to large track forecast errors if a recurvature from the S/PF to the M/MW pattern/region had been predicted.

A sequence of NOGAPS analyses during this transition from a S/PF to a S/EF pattern/region is given in Fig. 7. Notice first that the synoptic scenario is basically zonally oriented as in the S conceptual model (Fig. 4). Since this is a very early season TC, the subtropical anticyclone axis in Fig. 7a is relatively close to the Equator (about 17° S to west and about 13°S to the east). Consequently, the midlatitude westerlies have penetrated quite far north. A rather weak trough in the westerlies is passing to the south of the TC. Although a col region exists between the eastern and western subtropical anticyclone cells, it is clear in this case that this midlatitude trough is not penetrating far enough equatorward to cause a recurvature of the

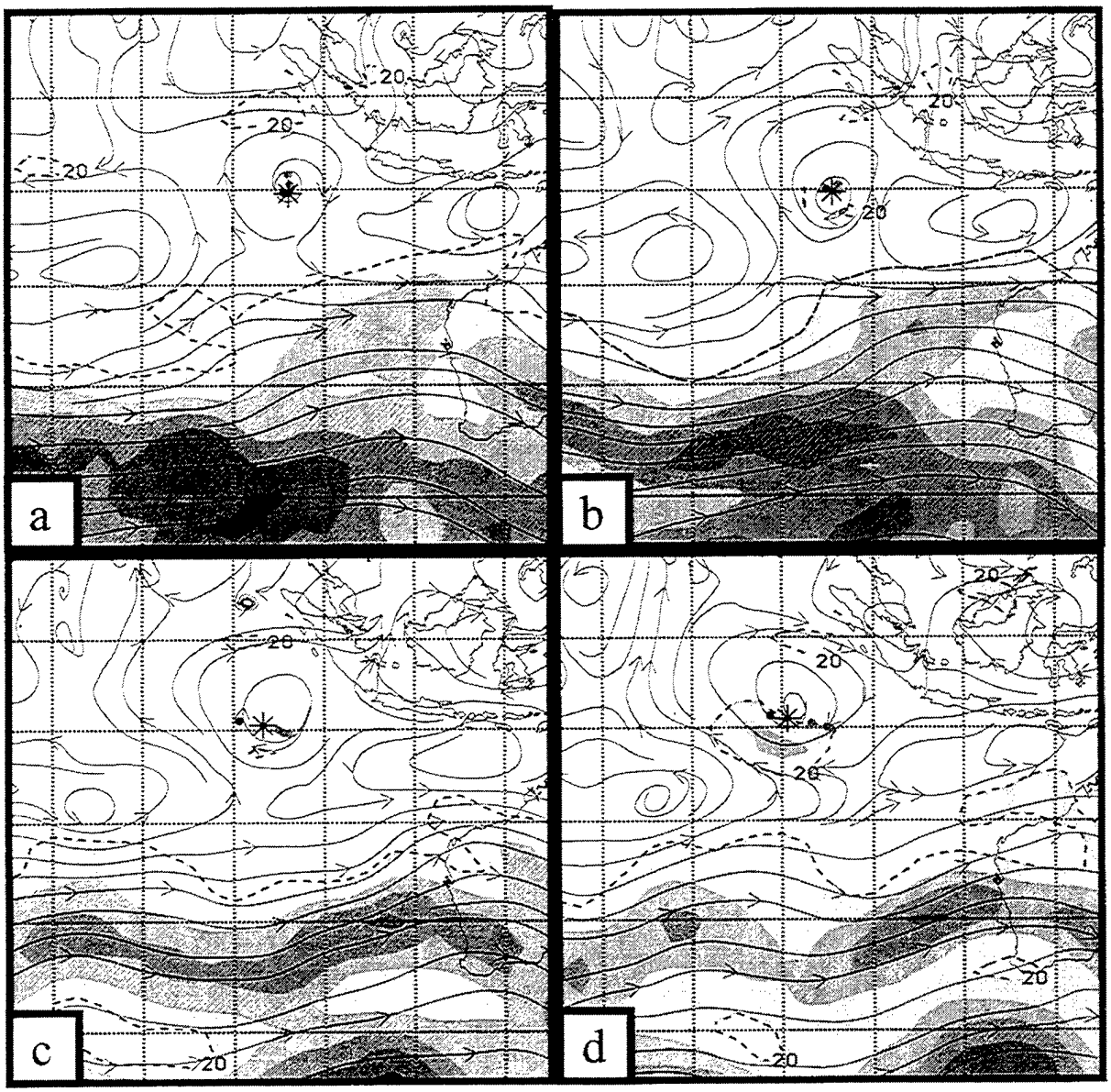

Fig. 7 NOGAPS 500-mb streamlines (thin solid lines) and isotachs (kt; dashed for 20 kt and then at 10-kt intervals) for TC Melanie/Bellamine at (a) 1200 UTC 30 October, (b) 0000 UTC 31 October, (c) 0000 UTC 1 November, and (d) 1200 UTC 1 November 1996. The present TC position is indicated by an asterisk and the -36, -24, -12, and + 12 h positions are indicated by dots.

TC. Because the steering flow in the col region is weak, Melanie/Bellamine is in the S/PF pattern/region and is drifting slowly (2 kt) toward 251°.

By 0000 UTC 31 October (Fig. 7b), Melanie/Bellamine is still in the col region with a weak midlatitude trough to the south. Notice that the western anticyclone has amplified and extended eastward somewhat. Two 20-kt isotach maxima are analyzed to the southeast and west of the TC. Although these isotach maxima are weak (and perhaps not oriented well relative to the streamlines), the implication is that the TC is being influenced by two steering flows. Whereas the larger 20-kt isotach that is to the southeast implies a southwestward steering flow, the narrow 20-kt isotach that is to the west implies an equatorward steering flow. Although moving only at 3 kt, Melanie/Bellamine has turned toward 291° (Fig. 6) so that the equatorward steering is becoming more dominant. That is, the TC is in a transition state from the S/PF to the S/EF pattern/region.

A new Midlatitude System Evolution (MSE) transitional mechanism (see Fig. 2, bottom left) is illustrated by the conceptual models in Fig. 8. One possible interpretation of this Melanie/ Bellamine case is that the Midlatitude Anticyclo-Genesis (MAG) transition (panel c → panel d) applies. In one form of this MAG transition, the translation of a midlatitude ridge is such that it becomes superposed on the subtropical ridge and causes an apparent modulation of the subtropical ridge, which changes the TC track. In the second mode of the MAG transition, actual subtropical anticyclogenesis (by physical mechanisms that are not well understood) occurs, and that amplification causes a steering flow change over the TC. Bannister et al. (1998) point out that modulation of the subtropical ridge by a midlatitude ridge or trough is a common occurrence in the Southern Hemisphere, and will often involve the intensification of the western

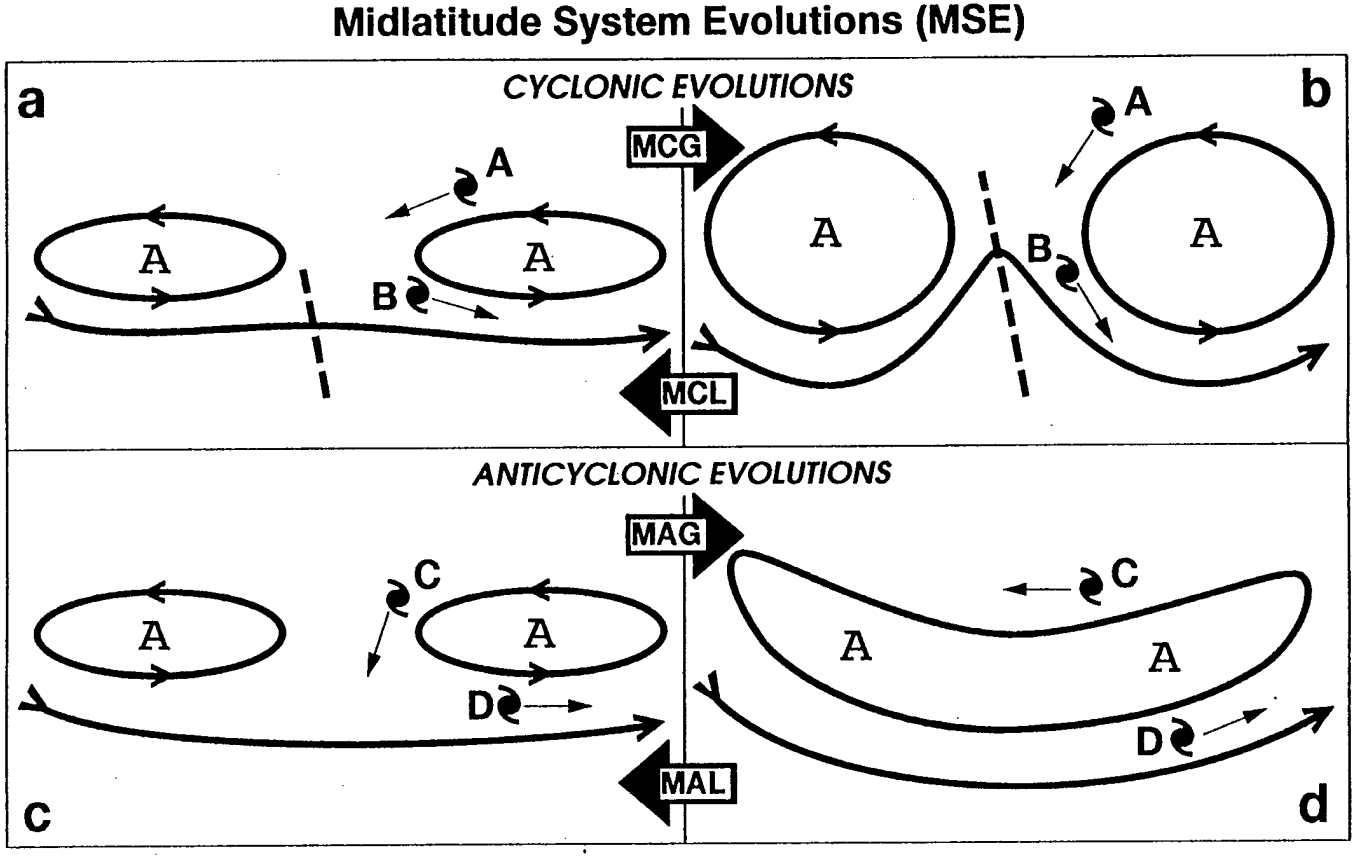

Fig. 8. Conceptual models of Midlatitude System Evolutions (MSE) that may affect the TC track. The deepening of the midlatitude trough from panel a to panel b depicts Midlatitude CycloGenesis (MCG) and the reverse order (panel b to panel a) implies Midlatitude CycloLysis (MCL). Similarly, the midlatitude anticyclone change poleward of TCC from panel c to panel d depicts Midlatitude AnticycloGenesis (MAG) and the reverse order (panel d to panel c) implies Midlatitude AnticycloLysis (MAL).

subtropical anticyclone. In their TC Betsy case study, Bannister et al. (1998) give an example of an amplifying subtropical anticyclone in which the anticyclogenesis is in response to Rossby wave dispersion from a high amplitude trough approaching from the west. Such a scenario does not apply in the Melanie/Bellamine case since at most a weak midlatitude trough is found at 60°E just to the left of the western edge in Fig. 7b.

Bannister *et al.* (1998) give other examples to illustrate that the Southern Hemisphere midlatitude westerlies and subtropical anticyclone may be considered to be more dynamically linked as troughs intrude equatorward and ridges push poleward. They give an example of TC Alexandra during December 1991 in which the track changes owing to the weakening of a midlatitude trough. In the new MSE conceptual model (Fig. 8), this transition would be considered a Midlatitude CycloLysis (MCL), which would be a circulation change from panel b to panel a. This MCL is an alternate interpretation for the Melanie/Bellamine case in that the already weak midlatitude trough to the south of the TC in Figs. 7a-b disappears during the next 24 h (Fig. 7c). Since the track change to the west is already evident at 0000 UTC 31 October (Fig. 7b), the MAG (versus a MCL) transition is favored in this Melanie/Bellamine case.

The more common Midlatitude CycloGenesis (MCG) transition in Fig. 8a-b is a typical cause of a TC recurving in advance of a midlatitude trough to the west. As in the MAG transition, the amplification due to the midlatitude trough may occur either through superposition via translation, or as a true cyclogenesis. Since such a scenario is well known, it will not be discussed further. A final alternative of Midlatitude AnticycloLysis (MAL) transition from panel d to panel c is the antithesis of MCG. A scenario in which the MAL transition might be applied is if the subtropical anticyclone establishing the steering flow over the TC decreases in amplitude for reasons other than the approach or amplification of a midlatitude trough.

During the MAG transition of Melanie/Bellamine in Fig. 7c, a single 20-kt isotach maximum is found to the south-southwest of the TC, which implies the primary steering flow is now attributed to the subtropical anticyclone to the southwest. In addition, Melanie/Bellamine is now moving toward 281°, and this equatorward of west motion is consistent with establishment of a S/EF pattern/region as in the S conceptual model in Fig. 4.

The circulation change resulting from the transition from S/PF to S/EF pattern/region is much clearer 12 h later (Fig. 7d) with a continuous subtropical anticyclone axis to the south of the TC along 17°S. A large 20-kt isotach with a 30-kt isotach maximum and the translation speed of 13 kt at 1200 UTC 1 November are consistent with the S/EF pattern.

As has been emphasized by Bannister *et al.* (1997, 1998) the Southern Hemisphere TC forecaster must be aware of the midlatitude circulations and the possible environment structure changes as in the MSE conceptual models in Fig. 8. Whereas the midlatitude influence on the western subtropical anticyclone in this Melanie/Bellamine case is rather subtle, in other cases the remote influence on the subtropical anticyclone will be more dramatic. Of course, a major consideration is the amplitude of the pre-existing subtropical anticyclone. In this (and many other Southern Hemisphere) case, the subtropical anticyclone was relatively weak and was more readily impacted than if the anticyclone was broad and of large amplitude. Perhaps a more typical example is that of the TC Daryl/Agnielle case described by Bannister *et al.* (1997; their section 6.b.2). Just as in this Melanie/Bellamine case, Daryl/Agnielle turns sharply from a poleward track to a westward track. In that case, the subtropical anticyclone had a broader meridional extent than in Fig. 7. Nevertheless, the midlatitude circulation change causing the MAG transition for Daryl/Agnielle was again not a large amplitude trough/ridge system. It is unclear how well the numerical weather prediction (NWP) models will be able to forecast such

subtle changes over the data-sparse Southern Hemisphere oceans. Evaluations of the large TC track error mechanisms in the dynamical models are in progress.

b. Changes in the Poleward (P) pattern

1. New P/EW pattern/region. A new Equatorial Westerlies (EW) synoptic region has been added in Fig. 4 to provide more flexibility in classifying TCs near the Equator while in a P synoptic pattern. Whereas this EW region is similar to the S/EW pattern/region, the difference is the northwest-to-southeast orientation of the monsoon trough and peripheral anticyclone in the P pattern compared to the zonally oriented monsoon trough and subtropical anticyclone with the intervening TE region in the S pattern (Fig. 4). Bannister *et al.* (1997; section 3b) describe the primarily poleward-oriented peripheral anticyclone to the east and give analysis examples of TCs in the P pattern.

One location where the P/EW region applies is in the South Pacific Convergence Zone, in which the monsoon trough does have a northwest-to-southeast orientation. However, the peripheral anticyclone, which is a product of Rossby wave dispersion, may not be well developed or may be absent. In such a case, the TC would be classified in the S/EW rather than the P/EW pattern/region. Given the requirement to also have the northwest-southeast oriented peripheral anticyclone present initially, TCs in the P/EW pattern/region are relatively rare. Furthermore, these eastward TC tracks (see arrow in Fig. 4) will be short because the time in the EW region is generally short as the TC quickly moves by the Advection transitional mechanism into the P/Poleward Flow pattern/region.

2. TC Usha case study. One case in which a P/EW classification may be applied is to a western TC that trails an eastern TC that has established the peripheral anticyclone. Such a case oriented existed at 0000 UTC 24 March 1994 for TC Usha moving eastward at 9 kt in an east-

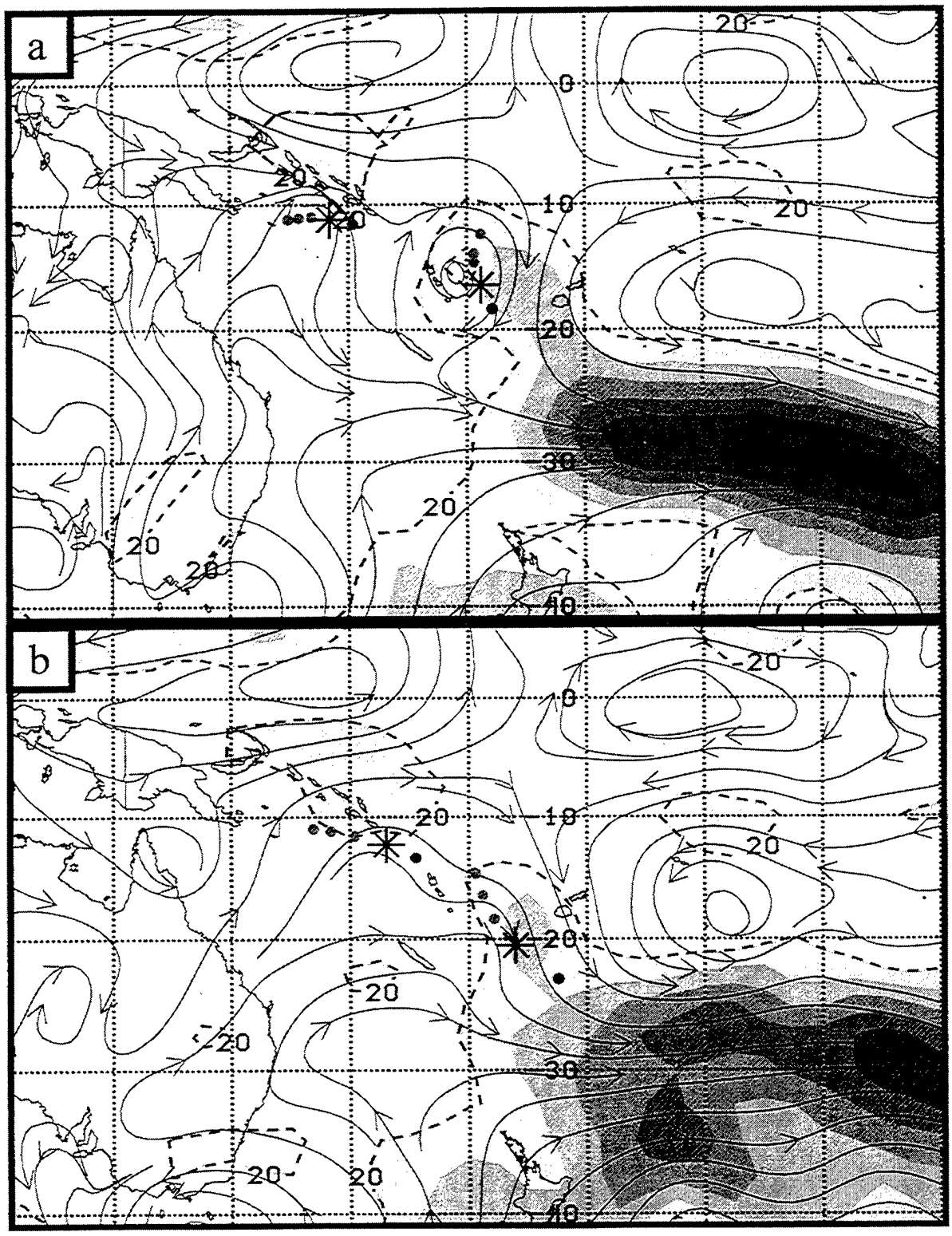

Fig. 9 NOGAPS streamline/isotach analyses as in Fig. 7, except at 0000 UTC on (a) 24 and (b) 25 March 1994 for (western) TC Usha and (eastern) TC Tomas.

west oriented monsoon trough (Fig. 9a). Meanwhile, TC Tomas to the southeast of Usha was already a well-developed storm moving south-southeastward. Notice the 30-kt isotach to the east of Tomas, which is consistent with a poleward steering flow. A peripheral ridge (anticyclone) northeast of Tomas connects the subtropical anticyclone to the east of Tomas and the equatorial buffer cell near 160°E north of Usha. On the larger scale, a midlatitude trough-ridge system to the south has displaced the eastern subtropical anticyclone toward the Equator (around 17°S).

By 0000 UTC 25 March (Fig. 9b), a 20-kt isotach is equatorward of TC Usha, which is now moving at 14 kt toward 108°. The conditions for the transition from the P/EW to the P/PF pattern/region are clearly established with the monsoon trough extending northwest to southeast to the west of Tomas. Similarly, the axis of the combined peripheral anticyclones of Usha and Tomas are also oriented northwest to southeast. Such a merger of the two peripheral anticyclones is a transitional mechanism called Reverse Trough Formation (RTF), which in this case re-enforces the P pattern. One of the symptoms of the peripheral anticyclone formation and intensification as part of the Rossby wave dispersion phenomenon is the associated subsidence. This subsidence is often revealed in satellite imagery by a clearing of the deep convection to the northeast (Southern Hemisphere) of the TC. Such a clearing is evident from 0300 UTC 24 March to 0300 UTC 25 March in the satellite infrared (IR) imagery (Fig. 10). Notice the linear orientation of the remaining deep convection and the clear regions to the east of the dateline.

During the next 12 h, TC Usha moved into the P/PF pattern/region (not shown) as it followed TC Tomas in the P pattern. Subsequently, a midlatitude trough deepened, and as Usha translated southeastward on the eastern flank of the trough, it completed a transition to the TP region of the H pattern (Fig. 4) (not shown).

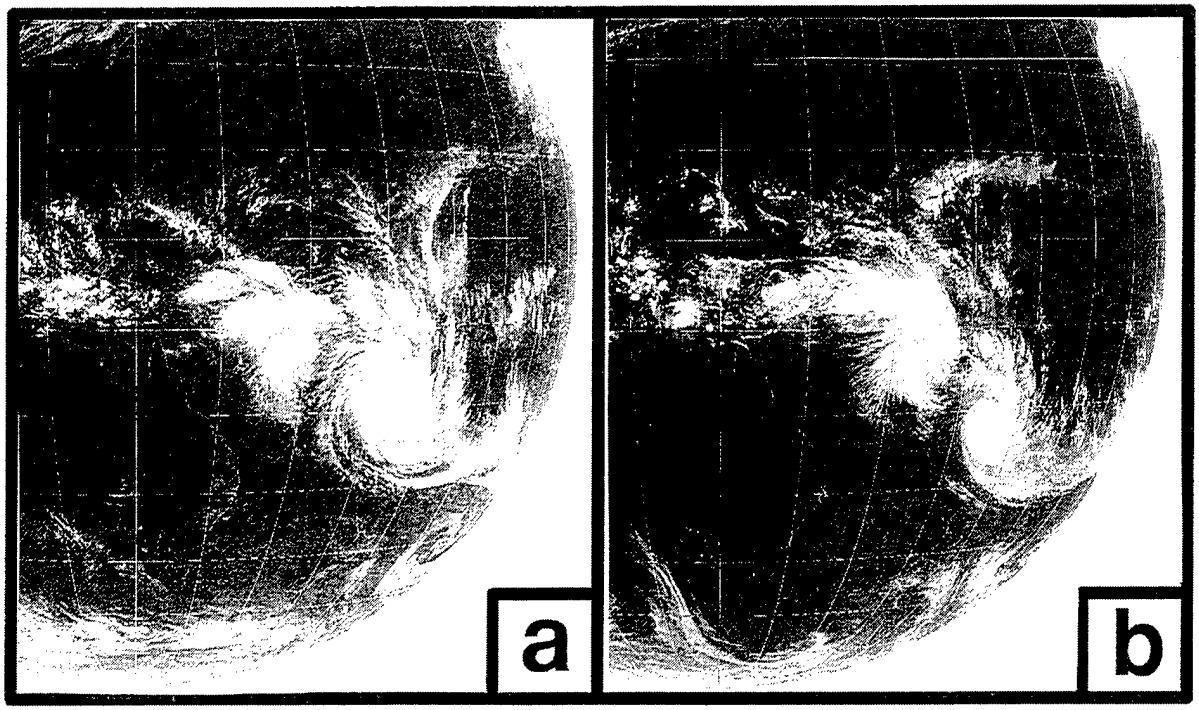

Fig. 10 Geostationary Meteorological Satellite infrared imagery at 0300 UTC on (a) 24 and (b) 25 March 1994 with TCs Usha and Tomas (southeastern TC).

3. New P/EF pattern/region. Another major change in the new P pattern conceptual model in Fig. 4 is the introduction of the Equatorward Flow (EF) synoptic region to the east of the peripheral anticyclone. Notice that an open TC symbol is used to emphasize that this is a different TC from the primary (western) TC that is generating the peripheral anticyclone via Rossby wave dispersion. It is when the steering flow of this eastern TC acquires a more equatorward component than would be expected that its synoptic pattern/region will now be classified as P/EF. In addition, the transitional mechanism for this track change of the eastern TC would have been listed as an Indirect TC Interaction (ITIE) as defined by Carr and Elsberry (1994) and Carr *et al.* (1997) for the western North Pacific. Bannister *et al.* (1997; section 5) describe the ITIE and an associated ITIW transitional mechanism, and provide examples.

In the transitional mechanisms in Fig. 2, the ITI mechanism is generalized to Indirect Cyclone Interaction (ICI). Schematics of the ICI transitional mechanism as it affects the eastern TC (ICIE) or the western TC (ICIW) are given in Figs. 11a and 11b, respectively. In the ICIW, the TC poleward steering flow attributed to its peripheral anticyclone is disrupted by the approach of a cyclone from the east. In the ICIE, the Rossby wave dispersion of a monsoon depression or a midlatitude trough to the southwest may generate a peripheral anticyclone that could deflect the eastern TC equatorward. Notice that the equatorward steering flow component owing to the peripheral anticyclone may not actually lead to a north of west track for a larger TC that has a sizeable poleward steering component associated with the beta-effect propagation.

4. Change in P/PF domain. Although a comparison of Figs. 3 and 4 might indicate only a re-naming of the previous Poleward-Oriented (PO) synoptic region to the PF region, a different interpretation has been made for TCs approaching the subtropical anticyclone axis. With the introduction of the Midlatitude (M) synoptic pattern (Fig. 4), and particularly its PF region, many TCs that had previously been kept in the P/PO pattern/region have now been classified as in the M/PF pattern/region. Bannister *et al.* (1998) had discussed the extended tracks of TCs in P/PO region (their Fig. 6) into the midlatitudes. Many of these TCs had actually passed through the subtropical anticyclone axis, but only the PO region option had been available in the P pattern. With the new P and M pattern conceptual models (Fig. 4), those TCs poleward of the subtropical anticyclone axis will now be classified as M/PF rather than P/PF, and the transitional mechanism (Fig. 2) listed as Advection.

5. TC Kristy case study. At 1200 UTC 11 March 1996 (Fig. 12a), TC Kristy with a intensity of 95 kt was coming ashore in Western Australia. Notice the large region enclosed by the 30-kt isotach to the east, which is consistent with the 8-kt translation toward 203°. The

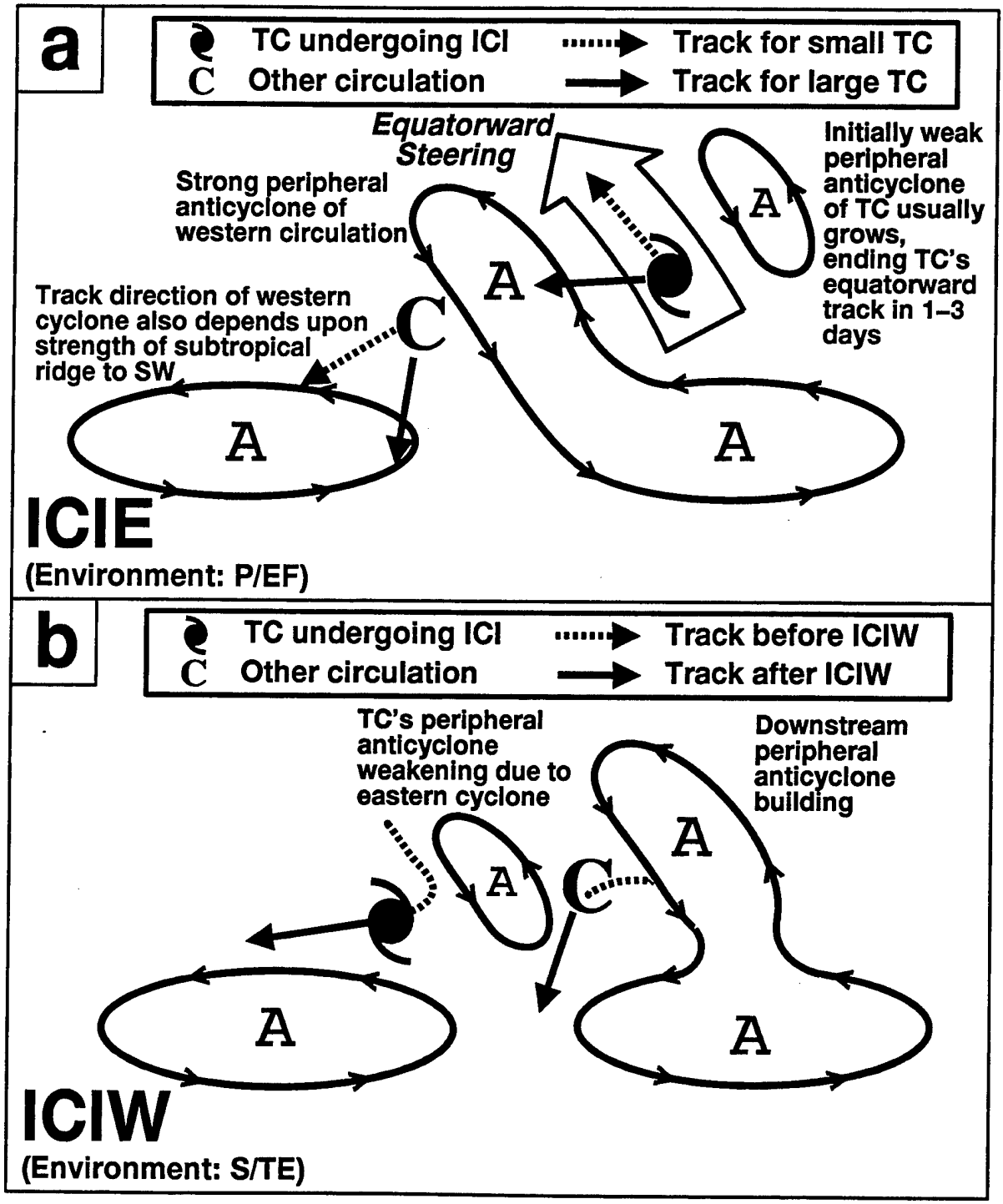

Fig. 11. Conceptual models as in Fig. 5a-b, except for Indirect Cyclone Interaction (ICI) transitional mechanism on the (a) eastern TC (ICIE) or (b) on the western TC (ICIW). The key circulation is the peripheral anticyclone trailing the western cyclone (or TC). In the ICIW, the approach of the eastern cyclone (or TC) diminishes the intervening anticyclone, and thus diminishes the poleward steering flow over the western TC, which may then turn westward in a transition from P/PF to S/TE. In the ICIE, the amplitude of the intervening anticyclone is growing or is maintained such that an equatorward steering flow is imposed on the eastern TC, which is then in the new P/EF pattern/region in Fig. 4.

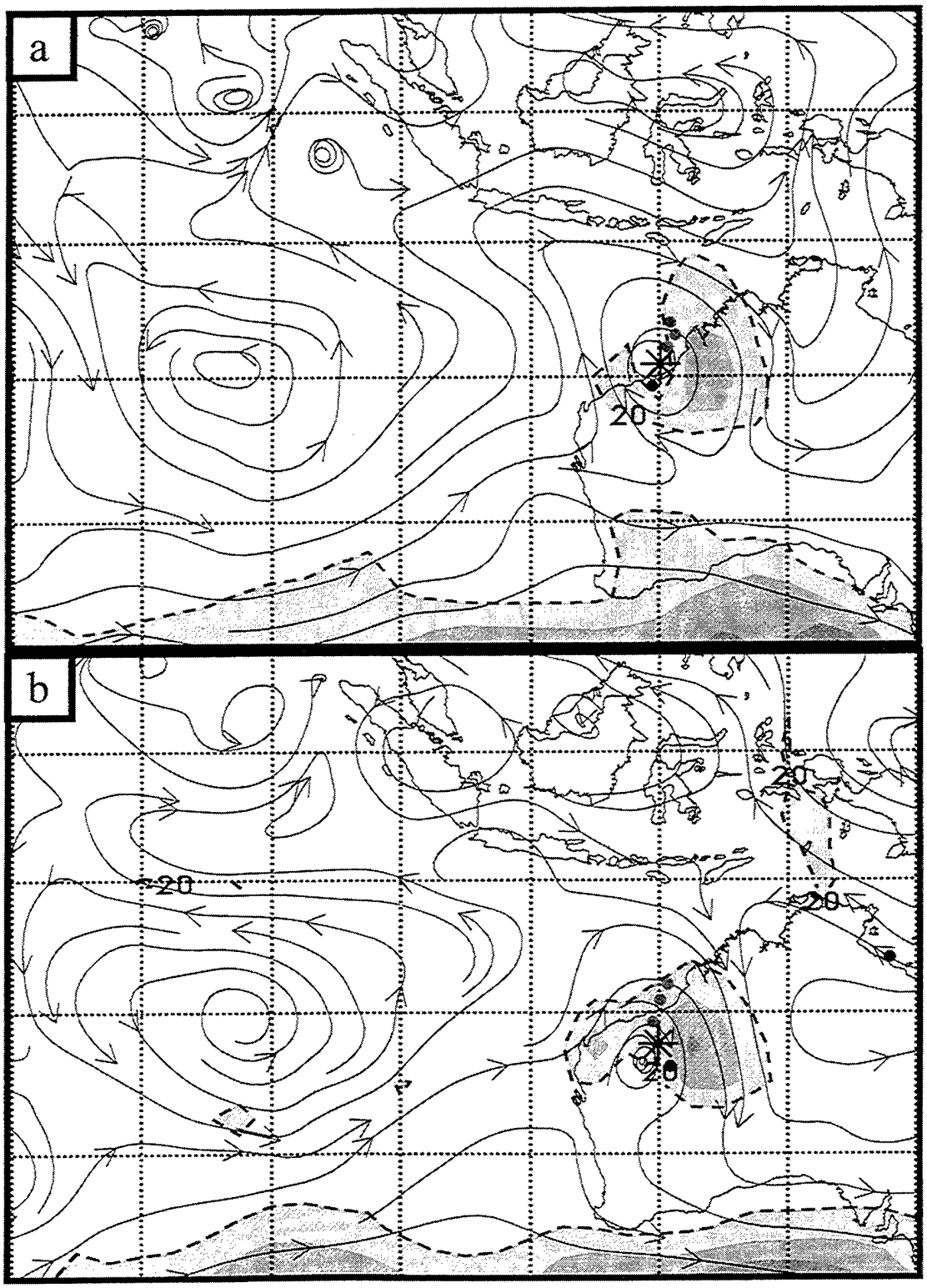

Fig. 12. NOGAPS streamline/isotach analysis as in Fig. 7, except for TC Kristy at 1200 UTC on (a) 11 and (b) 12 March 1996.

peripheral anticyclone blending with the eastern subtropical anticyclone, and its axis extending northward and then northwestward is a classical illustration of the P pattern. The existence and characteristics of this peripheral anticyclone are evidently supported by the frequent (6-h) radiosondes over Australia, and can not be argued to only be an artifact of a NWP center data assimilation technique that generates such peripheral anticyclones over data-sparse ocean regions.

After Kristy came ashore and quickly decreased in intensity (70 kt at 1200 UTC 12 March and 20 kt at 0000 UTC 13 March), the peripheral anticyclone also became less well-defined (Fig. 12b). Whereas the eastern subtropical anticyclone axis was obscurred by the peripheral anticyclone in Fig. 12a , the axis is clearly along 21°S, which is consistent with the subtropical anticyclone axis farther to the west. Consequently, this TC-environment situation is now classified as in a transition from the P/PF to the M/PF pattern/region, whereas using the old nomenclature Kristy had been classified as a P/PO pattern/region until it died.

c. New Midlatitude (M) synoptic pattern

Except for the High-amplitude (H)/Trough Poleward (TP) pattern/region, the new Midlatitude (M) pattern (Fig. 4) contains all TCs that are poleward of the subtropical anticyclone axis. Except for the Midlatitude Easterlies region, the environmental steering of the TC in the M pattern will have an eastward component. One of the reasons for this new M pattern is that Carr and Elsberry (1999) found distinctly different causes of large track errors by the numerical models depending on whether the TC is equatorward or poleward of the subtropical anticyclone axis. The reason the H/TP pattern/region is continued poleward beyond the subtropical anticyclone axis is that the steering flow of the TC is more attributed to the deep midlatitude trough rather than the subtropical anticyclone. In most cases, the TC in the H/TP pattern/region

will continue with a similar track direction and speed as it passes through the subtropical anticyclone axis. If a H/TP → M/PF transition had been enforced, a track direction and/or translation speed change would have been implied as in other transitions, which is not usually the case.

1. New M/PF pattern/region. Whereas a TC in the S pattern that recurved into the midlatitudes would have previously been classified directly in the Midlatitude Westerlies (MW) region (see Fig. 3), such a recurving TC will now be classified in the M/Poleward Flow (PF) pattern/region. In the previous terminology, movement into the MW region implied a translation speed increase as well as an eastward turn. The new M/PF pattern/region does imply an eastward turn, but not necessarily a large increase in translation speed. Indeed, movement along the southwestern flank of a more circular-shaped subtropical anticyclone than illustrated in Fig. 4 may be quite steady with only a slow eastward turn. If the TC in the M/PF region is still over relatively warm water, and is not exposed to large vertical wind shear, the TC may maintain intensity.

As indicated in section 2.b.4 above, several TCs that previously had been classified in the (old) P/PO pattern/region even beyond the subtropical anticyclone axis will now be said to have had a P/PF → M/PF transition. In the example (Fig. 12) of the transition of TC Kristy from the P/PF to the M/PF pattern/region, Kristy was dissipating over land. If the TC in the M/PF pattern/region is over relatively warm water, and is not experiencing large shear, the TC intensity may be sustained for some time, which may explain many of the long P/PO tracks into the midlatitudes in Bannister *et al.* (1998; their Fig. 6).

2. New M/MW pattern/region. Depending on whether the subtropical anticyclone is circular-shaped or has a narrow meridional extent as in Fig. 4, the TC in the PF region may then

experience a later or earlier, respectively, transition to the M/Midlatitude Westerlies (MW) pattern/region (Fig. 4) in which the motion will be more rapid eastward. This M/MW pattern/region is thus a subset of the prior S/MW pattern/region in Fig. 3. Since the environmental flow in the Southern Hemisphere midlatitudes tends to have large vertical wind shear, the TC may quickly dissipate. For these reasons, the number of TC tracks in the M/MW will be smaller than in the old S/MW combination, and will generally be shorter than in Bannister *et al.* (1998; their Fig. 5d).

3. New M/EF pattern/region. Although rarely observed, a TC in the M/MW pattern/ region may advect into the M/Equatorward Flow (EF) combination (Fig. 4), especially if the subtropical anticyclone builds meridionaly such that the TC is now on the southeastern flank and has a steering flow with an equatorward component. A midlatitude trough may also be to the east-southeast of the TC such that the vorticity advection behind the trough contributes to apparent meridional extension of the subtropical anticyclone.

4. New M/ME pattern/region. For consistency with other global TC regions, the M pattern in Fig. 4 includes a Midlatitude Easterlies (ME) region. No cases of TCs in the M/ME pattern/region have been found thus far in the Southern Hemisphere. Although a synoptic pattern with a separate midlatitude anticyclone poleward of the subtropical anticyclone has been observed, no TCs have either formed or moved into such a M/ME pattern/region. The Atlantic M/ME cases (Boothe *et al.* 1999) involved a late-season TC in which the subtropical anticyclone had been displaced toward the Equator. A TC could still form or be sustained in that case because the Atlantic ocean was still warm enough at the latitude of the trough or cyclonic shear zone between the subtropical and the midlatitude anticyclones. Perhaps the reason a TC has not

been observed in such a synoptic region in the Southern Hemisphere is that the sea-surface temperatures are not sufficiently high at comparable latitudes.

5. TC Celeste case study. The unusual track of TC Celeste is shown in Fig. 13. After moving slowly (4-5 kt) southwestward toward the Queensland coast in the S/PF environment with an intensity of 20-25 kt, Celeste became a tropical storm at 1200 UTC 26 January 1996 adjacent to the coast as the heading changed toward 166°. The track of Celeste is southeastward until 0600 UTC 27 January when the heading changed to 84°. By 1200 UTC 29 January, Celeste was moving toward 69° at 13 kt. However, Celeste then turned more eastward and decreased in intensity.

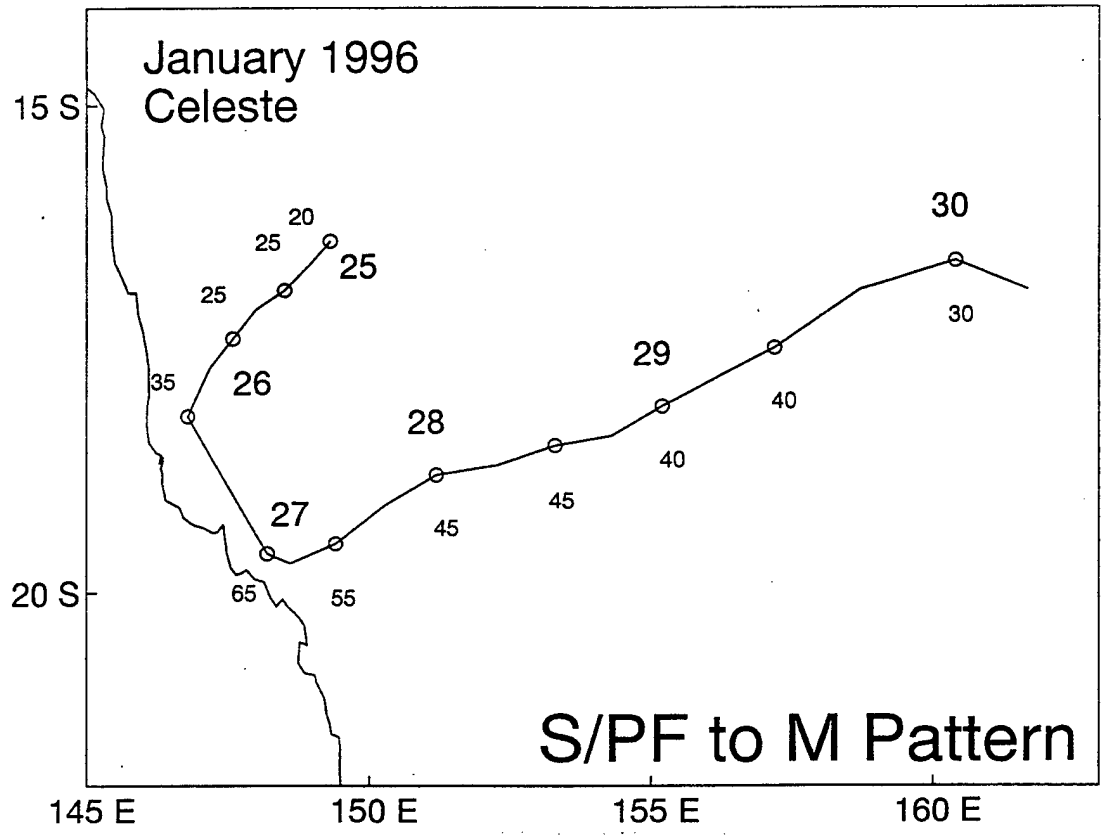

Fig. 13. Track as in Fig. 6, except for TC Celeste, and the small number is the intensity (kt).

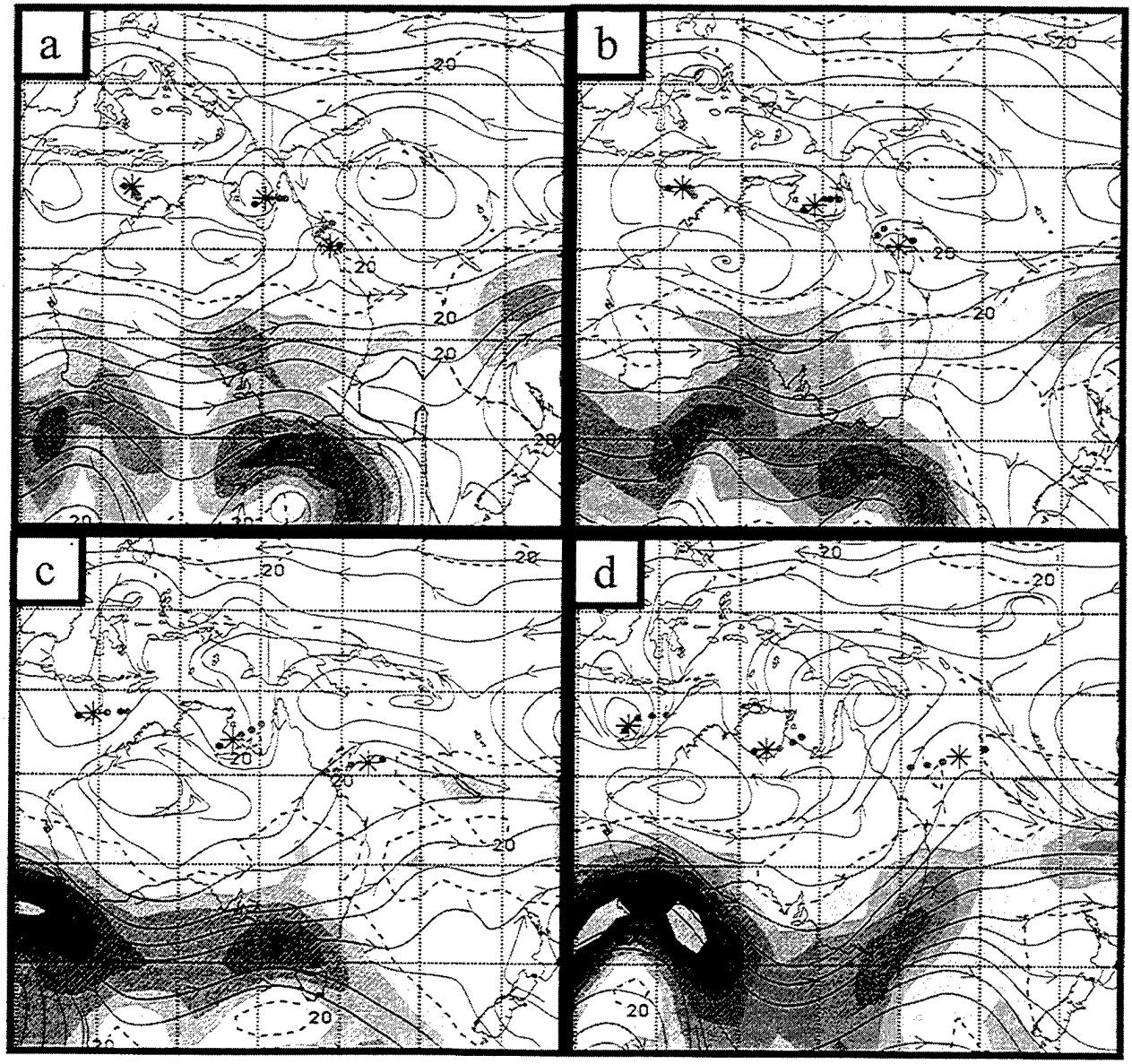

Fig. 14. NOGAPS streamline/isotach analyses as in Fig. 4, except at (a) 0000 UTC and (b) 1200 UTC 27 January 1996, and 1200 UTC on (c) 28 January and (d) 29 January for (eastern) TC Celeste. TCs Isobel and Jacob are to the northwest and north of Australia, respectively.

At 0000 UTC 27 January (Fig. 14a), Celeste is poleward of a tilted subtropical anticyclone axis that is along 20°S over Australia, but is north of 15°S over the western South Pacific. The elongated 20-kt isotach to the northeast of Celeste is an indication that the steering flow is toward the southeast which is consistent with the track (Fig. 13). That is, Celeste is in the M/PF pattern/region on the southwestern flank of the anticyclone to the northeast. Since the trough to the south-southwest is relatively weak, and the pattern is relatively zonal, this is not a High-amplitude (H) pattern.

After only 12 h (Fig. 14b), Celeste has begun to move eastward away from the east coast of Australia at a translation speed of 9 kt (Fig. 13). The midlatitude trough is passing directly south of TC, which is also poleward of the subtropical anticyclone. A more equatorward penetration of the midlatitude trough northeast of New Zealand appears to have contributed to a north-of-east tilt to the steering flow across Celeste. Notice the 20-kt isotach is rotating to be more equatorward of Celeste, which in addition to the overall synoptic pattern is an indication that Celeste is already in the M/MW pattern/region. The transitional mechanism in this case is Advection.

Twenty-four hours later (Fig. 14c), the general orientation of the steering flow continues to be north of east. Whereas the eastern subtropical anticyclone is displaced to almost 10°S, anticyclogenesis is occurring near 130°E over and south of Australia. Notice the 20-kt isotach is now on the western side of Celeste, which is moving toward 81° at 10 kt (Fig. 13). Thus, Celeste is in the M/EF pattern/region and a M/MW → M/EF transition has occurred via the Midlatitude AnticycloGenesis (MAG) transition as in Fig. 8 (panel c to panel d).

Eastward building of the western subtropical anticyclone is quite evident at 1200 UTC 29 January (Fig. 14d). Consequently, Celeste is on the southeastern flank of this western

anticyclone with a more equatorward steering flow. The 20-kt isotach is now to the southwest of the TC. However, the midlatitude trough-ridge system continues to move eastward (not shown). TC Celeste, which has now decreased in intensity to 30 kt, will soon turn to a more eastward motion (Fig. 13).

In summary, the new M synoptic pattern with the PF, MW, EF, and ME synoptic regions is consistent with midlatitude circulations in other global TC regions. It is convenient in that all TCs poleward of the subtropical anticyclone axis will be in the M pattern, except for the special case of the H/TP pattern/region. The PF, MW, and EF regions in the M pattern allow more flexibility in classifying the environment structure than the single S/MW pattern/region of Bannister *et al.* (1997, 1998). The new Midlatitude System Evolutions (MSE) conceptual models in Fig. 8 describe the two genesis (MCG and MAG) and two lysis (MCL and MAL) transitional mechanisms that may lead to pattern/region transitions, and thus TC track changes.

d. Changes in the High-amplitude (H) synoptic pattern

Thus far, the H synoptic pattern is unique to the Southern Hemisphere among the global TC basins, and is needed to represent the frequent intrusions of strong troughs and ridges into the low latitudes. Whereas the same four synoptic regions (Ridge Equatorward--RE, Ridge Poleward --RP; Equatorial Westerlies--EW; and Trough Poleward--TP) are found in Fig. 4 as in Fig. 3, the H pattern schematic in Fig. 4 has been changed. First, high-amplitude anticyclones have been included in Fig. 4 to the east and to the west of the deep, equatorward-penetrating trough. Two of these anticyclones may not always appear, and the single, high-amplitude anticyclone may be either to the west or to the east.

A second difference between Figs. 3 and 4 is that the RP region on the northwest flank of the eastern anticyclone has been drawn to connect with the TP region. This connection will

illustrate that a TC may form or move westward under the steering flow associated with the ridge into a steering flow attributed to the trough. In addition to illustrating possible TC formations in the RP region, the orientation and magnitude of the eastern anticyclone and the connectivity of the RP and TP regions are better represented in Fig. 4 than in Fig. 3. Whereas the RP region appears similar to the S/PF pattern/region in Fig. 4, the key difference is the more meridional (high-amplitude) anticyclone and trough circulation. An example of the H/RP $\rightarrow$ H/TP transition will be presented below.

A third difference between the H patterns in Figs. 3 and 4 is the connection of the RE and EW regions on the northeast flank of the western anticyclone in Fig. 4, which is intended to indicate two possible TC tracks. The TC may remain in the RE region and continue to move equatorward along the northeast flank, which was previously the only option (Fig. 3). In this scenario, the trough to the east may not have as large an equatorward penetration as the western anticyclone, so that the TC steering flow continues to be attributed to the anticyclone. The alternate TC track is a transition to the H/EW pattern/region, which results in a more northeastward track. In addition to connecting the RE and EW regions in Fig. 4 (versus a gap in Fig. 3), the curved track arrow in H/EW is intended to represent the possible track change following a H/RE $\rightarrow$ H/EW transition. This scenario becomes more likely if the trough to the east has a deep equatorward penetration. Since the majority of the TCs in the H/RE pattern/region seem to be influenced by vertical wind shear, and thus are relatively weak, the steering flow is typically better represented by the 700 mb analysis than by the 500 mb analysis.

1. TC Karlette case study. At 0000 UTC 23 February 1997 (Fig. 15a), TC Karlette is at 23.2°S, 58.4°E and is moving toward 217° at 11 kt. Notice that Karletta is on the northwestern flank of a deep anticyclone with a deep midlatitude trough approaching from the west. The 30-kt

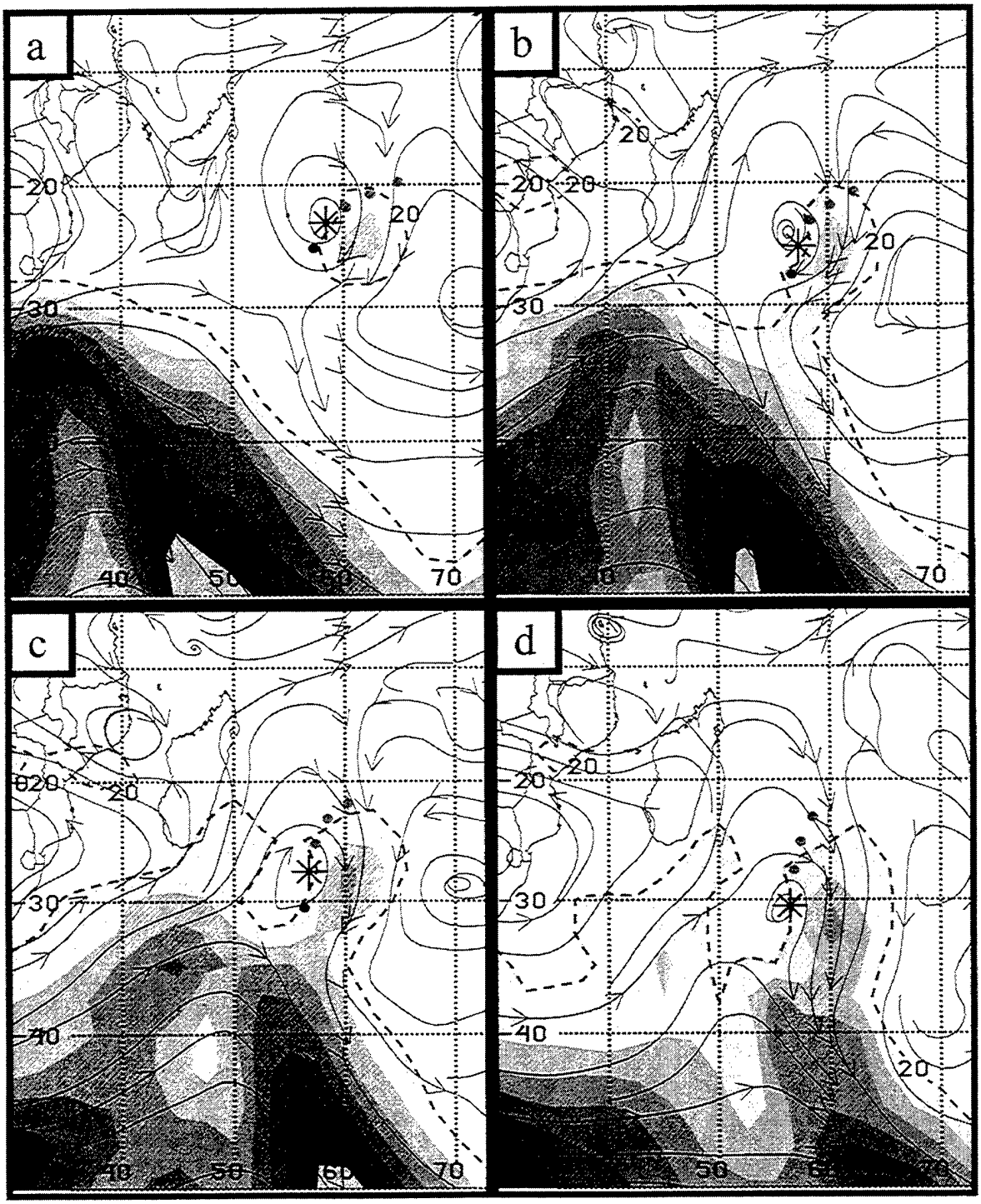

Fig. 15. NOGAPS streamline/isotach analyses as in Fig. 4, except at (a) 0000 UTC and (b) 1200 UTC 23 February and (c) 0000 UTC and (d) 1200 UTC 24 February 1997 for TC Karlette.

isotach maximum is to the southeast, which is consistent with the southwestward steering motion, and the classification in the H/RP pattern/region.

By 1200 UTC 23 February (Fig. 15b), TC Karlette is moving at 12 kt toward 197°. A Midlatitude Cyclo-Genesis (MCG) transitional mechanism (Fig. 8 panel a to panel b) is clearly operating as the midlatitude trough axis is now near 44°E. However, Karlette is still clearly in the H/RP pattern/region on the northwest flank of the deep eastern anticyclone to the east, which has an axis with a meridional extent from 10°S to 50°S. Notice that the 30-kt isotach is still to the southeast, which indicates a steering flow controlled by the eastern anticyclone.

The deep midlatitude trough is near 49°E between 30°S and 50°S by 0000 UTC 24 February (Fig. 15c), and an equatorward extension of the trough is apparent as a 20-kt isotach is now analyzed to the west of Karlette. However, the isotach maximum on the eastern side has increased to 40 kt, which indicates the eastern anticyclone is still the primary factor in the steering flow over Karlette. At this time, Karlette is moving at 12 kt toward 190°. With this translation direction, and the continued approach of the midlatitude trough, Karlette is considered to be in a transitional state between the H/RP and the H/TP pattern/region.

Karlette is embedded in the midlatitude trough circulation at 1200 UTC 24 February (Fig. 15d). The translation speed has increased to 18 kt toward 175°. Consequently, the H/RP → H/TP transition is complete. The intensity of Karlette was evidently being influenced by vertical wind shear as the midlatitude trough approached, with a decrease from 60 kt to 45 kt over the 36-h period of Fig. 15.

2. TC Roger case study. Whereas Roger had previously been drifting southward, at 0600 UTC 17 March 1993 the translation of Roger slowed to 2 kt with a turn toward 90°. Roger then began an extended northeastward track before turning to the southeast (121° at 4 kt) at 1200

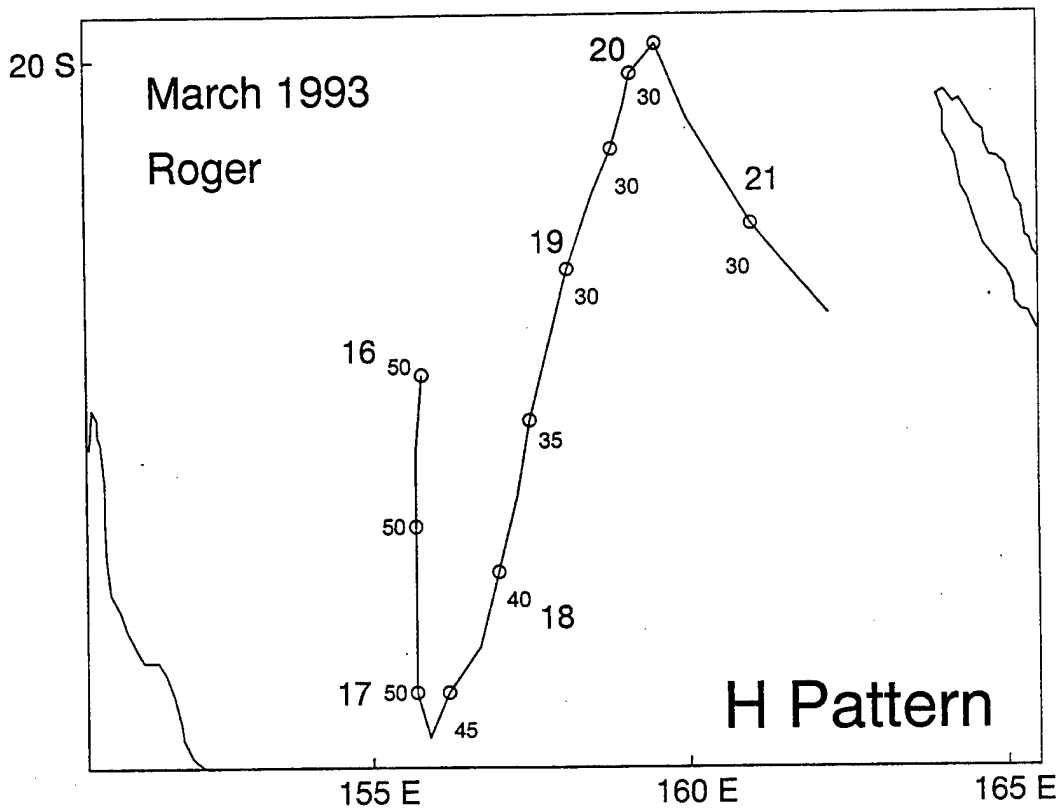

Fig. 16. Track as in Fig. 13, except for TC Roger.

UTC 20 March. This track is clearly non-climatological. Since TC Roger had an intensity of 45 kt at 12 UTC 17 March and decreased to 30 kt by 18 UTC 18 March, analyses at 700 mb (Fig. 17) are appropriate for describing this H/RE → H/EW transition. Although only a small portion of the analysis domain is displayed in Fig. 17, the circulations from 90°E to 160°W had a meridional character with northwest-southeast tilts of the troughs and ridges that extended equatorward to 10°S.

Prior to 17 March, Roger had been in a weak H/TP pattern/region. At 1200 UTC 17 March (Fig. 17a), Roger is in a col region between two anticyclones with isotach maxima to the southwest and to the northeast. Since a small 30-kt isotach and a larger 20-kt isotach is to the southwest, the anticyclone to the southwest has become the primary circulation determining the steering flow over Roger. Consequently, the environment of Roger is classified in the H/RE

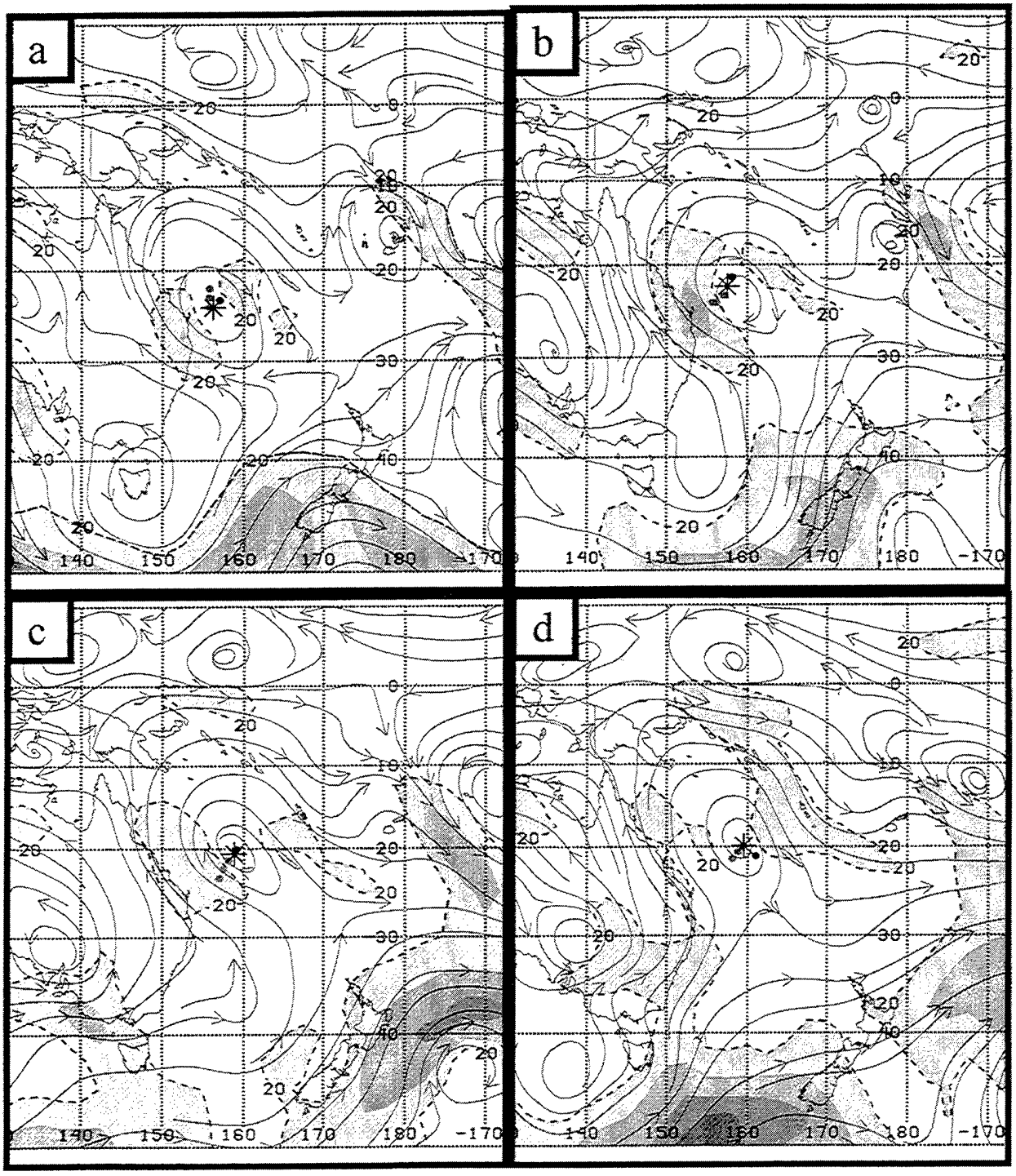

Fig. 17. NOGAPS streamline/isotach analysis as in Fig. 7, except at 700 mb and for TC Roger at 1200 UTC on (a) 17, (b) 18, (c) 19, and (d) 20 March 1993.

pattern/region of Fig. 4. The strengthening of the western anticyclone occurs in conjunction with a Midlatitude Anticyclo-Genesis (MAG) transitional mechanism as in Fig. 8 (panel c → panel d) over southeastern Australia and Tasmania. Satellite imagery (not shown) reveals an extensive, coincident area of subsidence with stratocumulus. The midlatitude trough over New Zealand is also amplifying at this time.

The dominance of the western anticyclone is quite evident at 1200 UTC 18 March (Fig. 17b), with an extensive 20-kt isotach region and a larger 30-kt isotach region than had been present 24 h earlier (Fig. 17a). Roger is now moving toward 24° at 6 kt. As Roger is approaching the apex of the trough, a transition to the H/EW pattern/region is considered to be possible.

The synoptic situation is similar 24 h later (Fig. 17c), except the amplitude of the anticyclone to the west and south has diminished. A weakening of the steering flow over Roger is indicated by the reduction of the magnitude and areal extent of the isotach maximum to the west. Roger has continued to drift (4 kt) toward the northeast (heading of 37°). Thus, Roger is still in a transition between the H/RE and H/EW pattern/region.

At 1200 UTC 20 March (Fig. 17d), the anticyclone (ridge) to the south of Roger has been replaced by a rapidly moving midlatitude trough, which is a reflection of the Midlatitude Cyclo-Genesis (MCG) transitional mechanism (Fig. 8 panel a → panel b). With the weakening of the anticyclone to the west, and thus a reduction of the western isotach maximum, the ridge (anticyclone) to the east becomes the primary steering flow influence. Roger turns toward 121° and is moving at 4 kt. Even though Roger might then be classified in the H/EW pattern/region, the isotach maximum was not analyzed to the north of the TC as in the conceptual model in Fig.

4. Twelve hours later, Roger had increased in translation speed to 12 kt with a heading toward 122° (Fig. 16) in the H/TP pattern/region.

3. 1991-99 environment structure and transition climatology

a. *Environment structure*

With the addition of 11 TCs in the South Indian Ocean and the 14 TCs in the South Pacific Ocean during the 1998-99 season, the numbers of TCs in the 1991-99 sample are 161 and 101, respectively. The environmental structure data base of 12-h synoptic pattern/region classifications totals 2339 and 1284, respectively. Thus, the Southern Hemisphere data base has increased to 3623 cases, whereas Bannister *et al.* (1998) had a sample of 3257 cases during 1991-98. The purposes here are to summarize the statistics of this expanded sample whenever the TC is in a single pattern/region (i.e., not in a transition condition) in Fig. 4, and to describe the significant changes from the old environment structure in Fig. 3.

Although the Standard (S) pattern still applies in 53.7% of the 2731 cases, an unequal distribution occurs with 1136 of the 1787 cases (63.6%) in the South Indian Ocean and only 331 of the 944 cases (35.1%) in the South Pacific (Fig. 18). The latter number is a major change from the Bannister *et al.* study in which 55.2% of the South Pacific cases were in the S pattern. This major change arises mainly by re-classifying many of the S cases to be in the new Midlatitude (M) pattern (209 of the 944 South Pacific cases, or 22.1%). Introduction of the M pattern also decreased the percentages of cases in the Poleward (P) pattern: 17.6% (15.8%) in the South Indian (Pacific) Ocean versus 19.1% (18.7%) in the Bannister *et al.* study. Finally, the High-amplitude (H) pattern now includes 11.3% and 27.0% of the cases in the South Indian and South Pacific Oceans, respectively. Thus, a somewhat more balanced distribution among the four synoptic patterns exists in the South Pacific Ocean, with a range between 35.1% in the S pattern to 15.8% in the P pattern. By comparison, the range in the South Indian Ocean is from 63.6% in the S pattern to only 7.5% in the M pattern. The various differences among the patterns

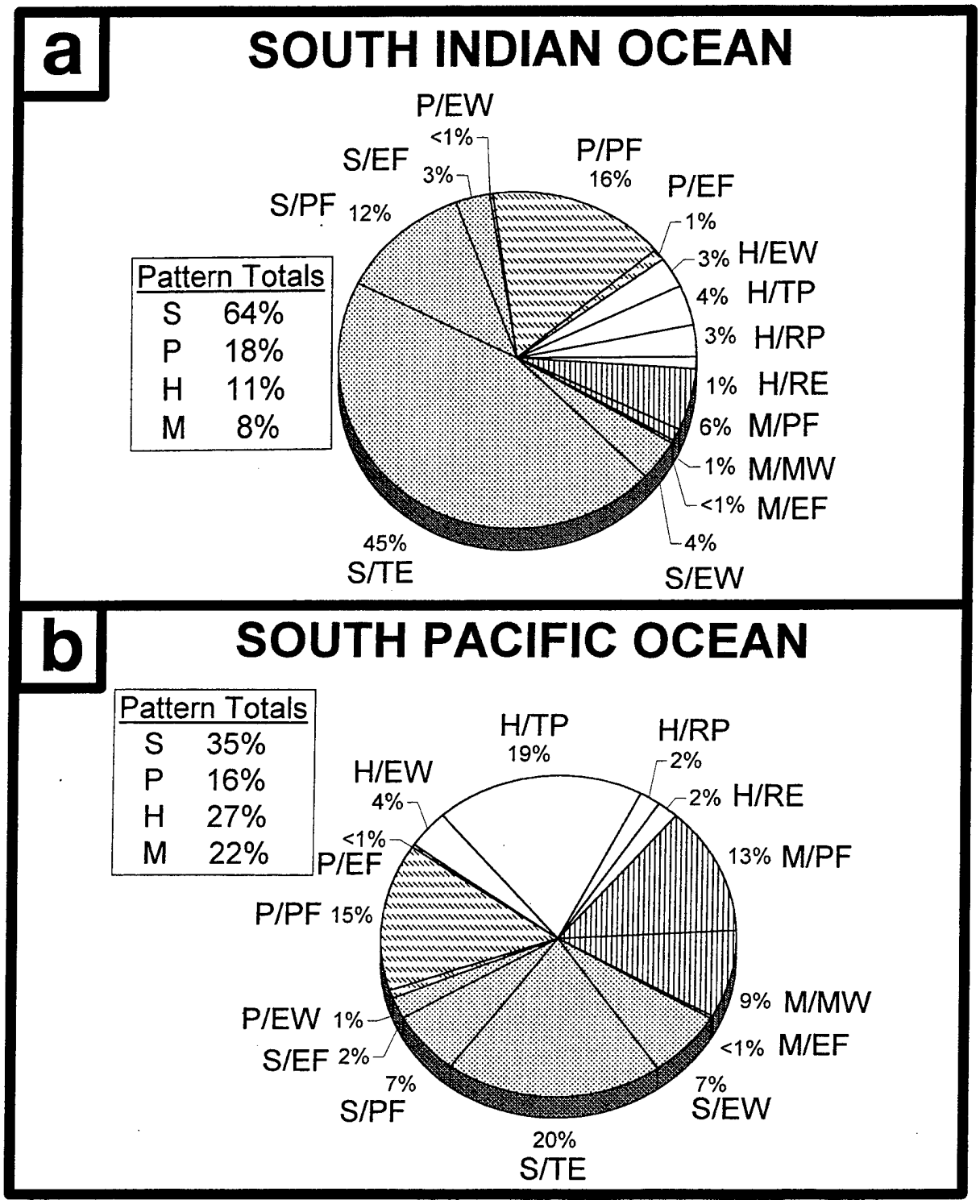

Fig. 18. Percent of synoptic pattern/regions in the 12-h analyses for (a) 2339 cases in the South Indian Ocean and (b) 1284 cases in the South Pacific Ocean during the 1990-91 through 1998-99 seasons.

in the two basins will be described further below with respect to the distributions of synoptic regions within these patterns, as shown in Fig. 18.

1. Standard (S) pattern. The dominance of the S pattern in the South Indian Ocean (Fig. 18a) is obvious, with 44.5% of all cases in the Tropical Easterlies (TE) region alone. Another frequent synoptic region in the South Indian S pattern is the Poleward Flow (PF) region with 11.7% of the cases in that basin. The comparable Weakened Ridge (WR) region in the S pattern (see Fig. 3) in the Bannister *et al.* (1998) study had only 5.4% of the South Indian cases. The larger number in the S/PF pattern/region reflects the new interpretation of the PF region as having an earlier poleward turn of the TC. By contrast, the TE and PF regions in the South Pacific (Fig. 18b) S pattern include 19.7% and 6.7% of the cases, respectively. This contrast is well illustrated in the track summary for the S pattern in Fig. 19. Notice the relatively small number of S/TE tracks in the South Pacific compared to the number in the South Indian Ocean. Many of these tracks continue westward for some distance, as would be expected for a TC on the equatorward side of the subtropical anticyclone (Fig. 4). By contrast, the S/PF tracks are mainly short segments in both basins, although some longer segments occur in the South Indian Ocean.

The tracks in the other two synoptic regions of the S pattern are also shown in Fig. 19. The Equatorial Westerlies (EW) region tracks in the South Indian Ocean are almost unchanged from the prior Bannister *et al.* (1998) study. Some reclassifications of the S/EW cases in the South Pacific Ocean resulted in a decrease from 12.3% in the Bannister *et al.* study to 6.8% in this study. The new Equatorward Flow (EF) region in the S pattern has almost exclusively short track segments (Fig. 19d), which indicates that the TC remains in this region for only brief periods. Recall the arrangement with two TCs in the SCIW transitional mechanism in Fig. 5a. In that scenario, the western TC in the EF region is only temporarily in a favorable position relative

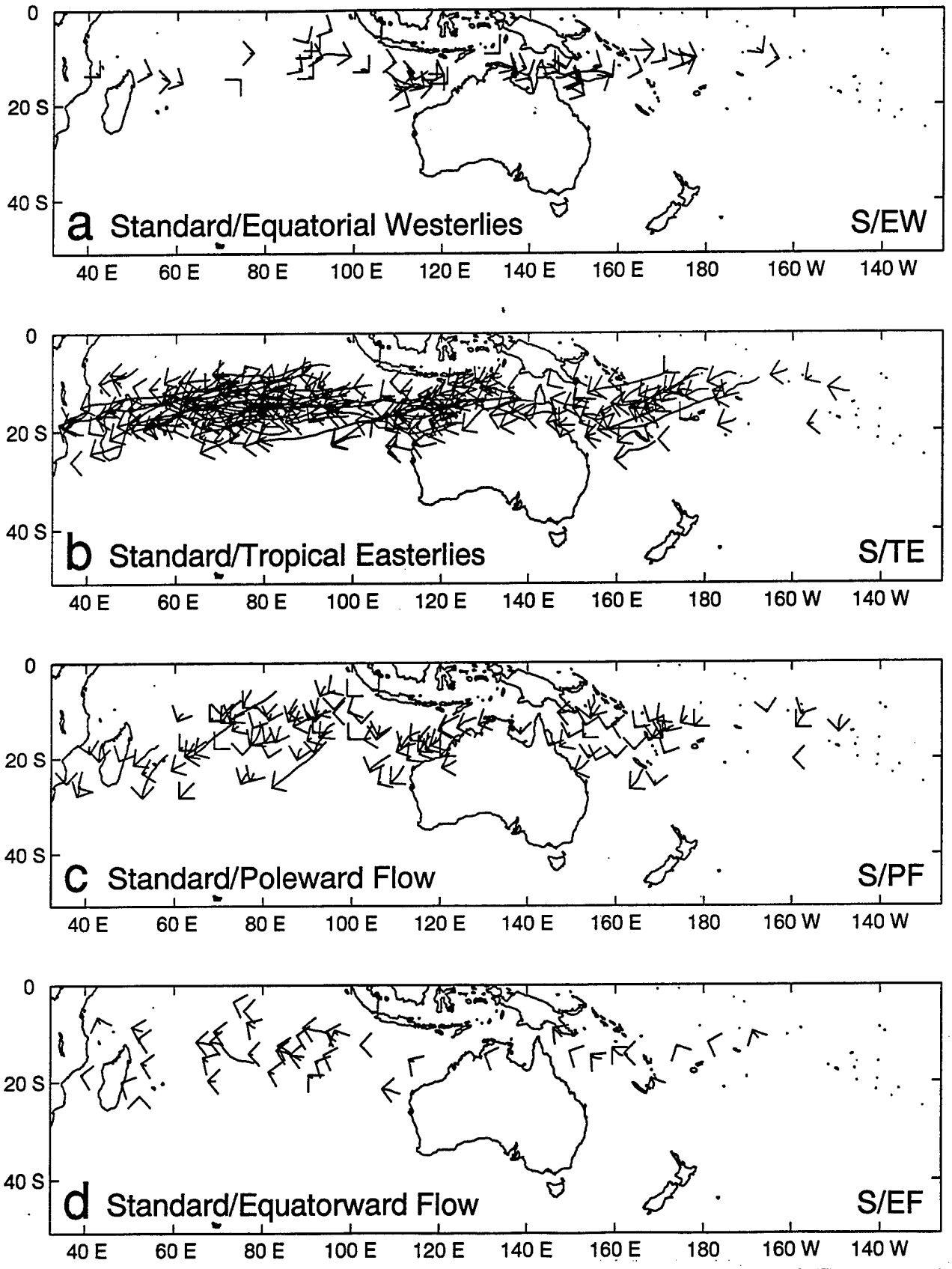

Fig. 19. Tracks of TCs during the 1990-91 through 1998-99 seasons while in the Standard (S) pattern and Equatorial Westerlies (EW), Tropical Easterlies (TE), Poleward Flow (PF), or Equatorward Flow (EF) regions. The ending position is indicated with an arrow.

to the eastern TC in the PF region, because the equatorward (poleward) motion of the western (eastern) TC will end the SCIW mechanism. Another scenario for a TC in the S/EF pattern/region is following a failed recurvature when the midlatitude trough has translated eastward and the TC is exposed to an equatorward steering flow component behind the trough. This situation persists for a short time before a more westward track in the S/TE pattern/region is established.

2. Poleward (P) pattern. As noted above, the overall percentages of cases in the P pattern are about the same with 17.6% in the South Indian and 15.8% in the South Pacific Ocean. The dominant synoptic region in the P pattern is the PF region with 16.2% in the South Indian (Fig. 18a) and 14.8% in the South Pacific (Fig. 18b). The tracks while the TC is in the P/PF pattern/region (Fig. 20) are very similar to those in the P/Poleward-Oriented (PO) pattern/region of Bannister *et al.* (1998, their Fig. 6). One notable difference is that the P/PF tracks (especially in the South Pacific) terminate at lower latitudes than did the P/PO tracks. This is a result of the new Midlatitude (M) pattern (Fig. 4), which applies whenever the TC has passed through the subtropical anticyclone axis. Thus, many of the long poleward tracks in the old P/PO pattern/region are now reclassified as being in the M/PF pattern/region (see later Fig. 21) after they pass through the subtropical anticyclone axis.

The new P/Equatorial Westerlies (EW) pattern/region has very few cases with only 0.3% in the South Indian Ocean (Fig. 18a) and only 0.7% in the South Pacific Ocean (Fig. 18b). As shown by the tracks in Fig. 20, almost all of the P/EW cases occur as the TC is approaching the South Pacific Convergence Zone area, and most of these TCs will then move poleward in the P/PF pattern/region. The only two cases in the South Indian Ocean are near the east coast of Africa in the Mozambique Channel.

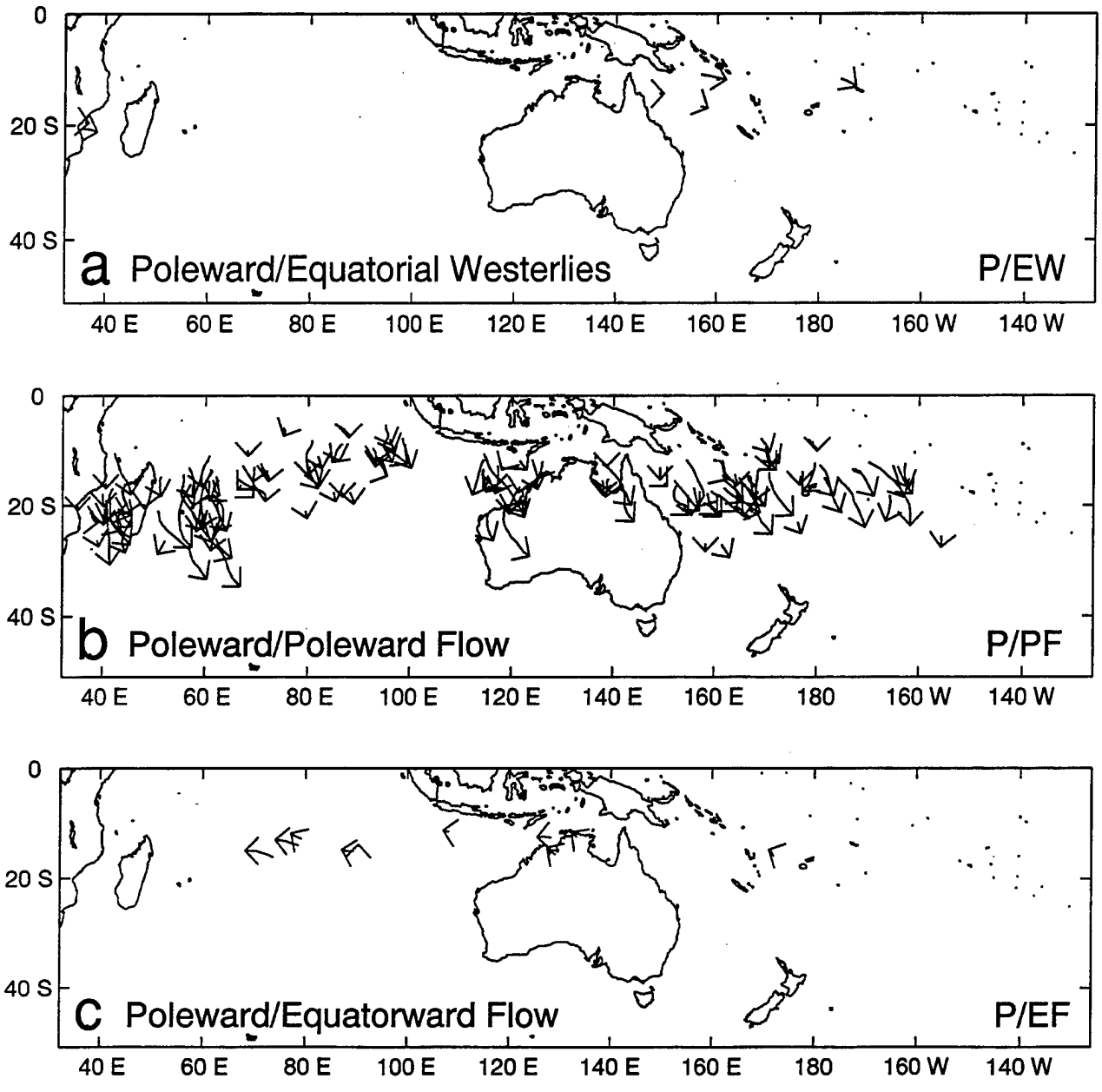

Fig. 20. Tracks as in Fig. 19, except in the Poleward (P) pattern and Equatorial Westerlies (EW), Poleward Flow (PF), and Equatorward Flow (EF) regions.

Similarly, the percentages of cases in the new P/Equatorward Flow (EF) pattern/region are small: 1.1% in the South Indian Ocean (Fig. 18a) and 0.2% in the South Pacific (Fig. 18b). Recall from Fig. 4 that this P/EF pattern/region typically applies when the TC is to the east of a peripheral anticyclone associated with a cyclone to the west, or a western TC in the P/PF pattern/region. More generally, a TC in the P/EF pattern/region is by definition the eastern TC in the Indirect Cyclone Interaction (ICIE) transitional mechanism (Fig. 11a). In most cases, this is a transient scenario because of the differential equatorward (poleward) motion of the eastern (western) TC (cyclone). Almost all of the P/EF cases in this sample occur in the South Indian Ocean, with only one case in the South Pacific Ocean (see tracks in Fig. 20).

3. High-amplitude (H) pattern. As emphasized by Bannister *et al.* (1997, 1998), the H pattern is a unique environment structure that is especially important in the South Pacific (27% of all cases). The most commonly occurring synoptic region in the H pattern is the Trough Poleward (TP) region (Fig. 4) in which the TC moves poleward (often rapidly) under the steering influence of a deeply penetrating midlatitude trough. Whereas the H/TP pattern/region accounts for 19% of all the cases in the South Pacific (Fig. 18b), it accounts for only 4.3% of the South Indian Ocean cases (Fig. 18a). Although this percentage difference is somewhat evident in the larger number of H/TP tracks in the South Pacific in Fig. 21, a considerable number of H/TP tracks also occur in the South Indian Ocean. The smaller percentage in the South Indian Ocean is also because of the larger number of TCs and environment structure classifications in that basin relative to the South Pacific.

The H/Equatorial Westerlies (EW) pattern/region is essentially unchanged relative to the Bannister *et al.* (1998) study. Only 3.2% (4.1%) of the cases in the South Indian (Pacific) Ocean

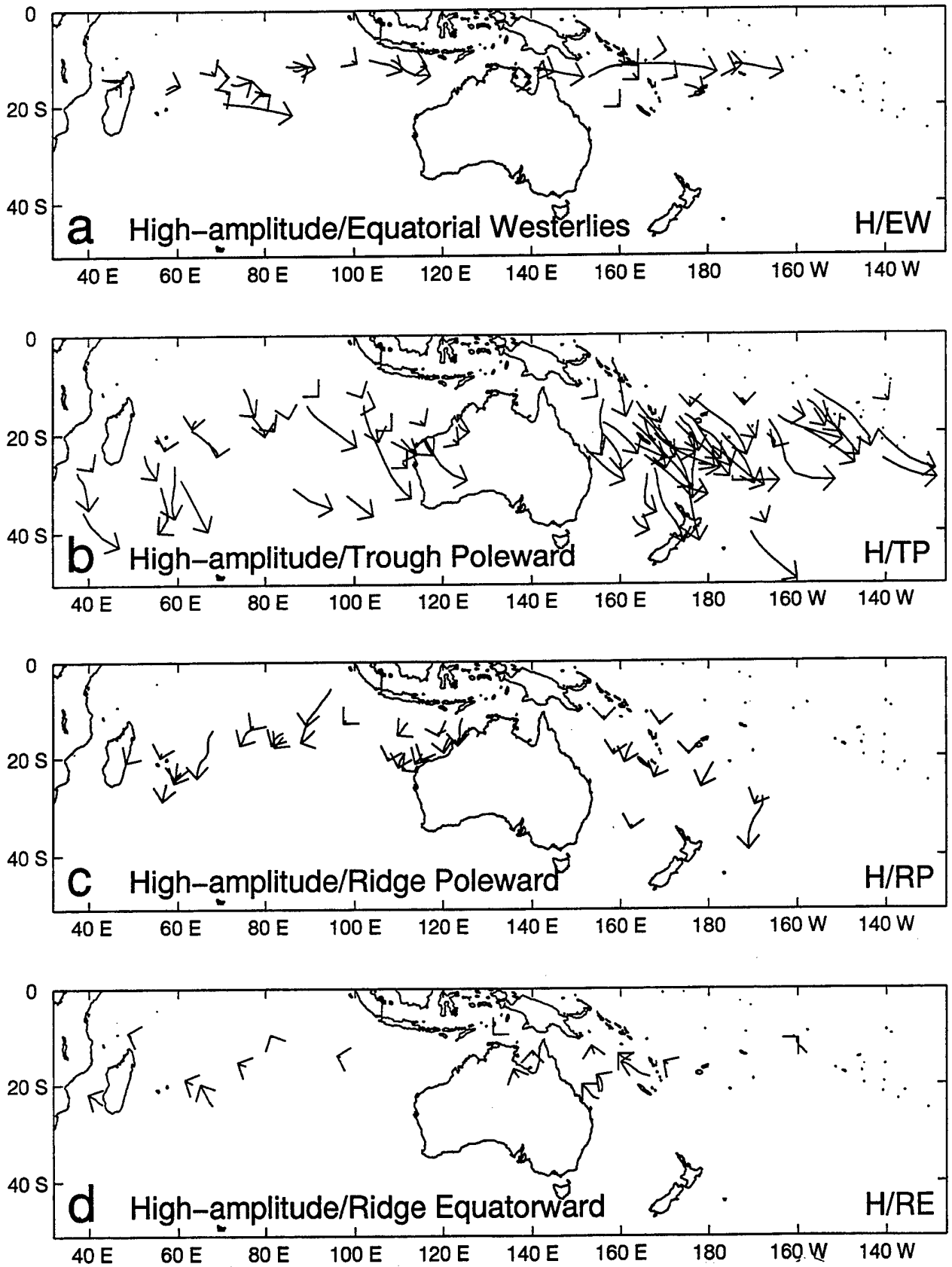

Fig. 21. Tracks as in Fig. 19, except in the High-amplitude (H) pattern and Equatorial Westerlies (EW), Trough Poleward (TP), Ridge Poleward (RP), and Ridge Equatorward (RE) regions.

are in the H/EW pattern/region (Fig. 18). The H/EW tracks in Fig. 21 are almost the same as in Bannister *et al.* (1998; their Fig. 7c).

Similarly, the H/Ridge Equatorward (RE) pattern/region is essentially unchanged relative to the Bannister *et al.* study. This relatively rare (0.9%) in Southern Indian Ocean and 2.0% in the South Pacific -- see Fig. 18) pattern/region has anomalous equatorward tracks (Fig. 21) that are generally short segments.

Finally, the H/Ridge Poleward (RP) pattern/region is also little changed from the Bannister *et al.* (1998) study. Only 2.9% (1.9%) of the cases in the South Indian (Pacific) Ocean (see Fig. 18) are in the H/RP pattern/region. The generally southwestward tracks as the TC moves in the steering flow around the eastern anticyclone in the H/RP pattern/region (Fig. 21) are again similar to the Bannister *et al.* (1998; their Fig. 7b) study.

4. Midlatitude (M) pattern. The major change in the new environment structure (Fig. 4) is the introduction of the M pattern, which accounts for 7.5% (22.1%) of the cases in the South Indian (Pacific) Ocean. The predominant synoptic region in the M pattern is the Poleward Flow (PF) region, with 5.8% (12.9%) of the cases in the South Indian (Pacific) Ocean (Fig. 18). As indicated in section 3.a.2 above, many P/PF cases have been reclassified as M/PF cases as the TC passed poleward through the subtropical anticyclone axis. In the Bannister *et al.* (1998) conceptual model (Fig. 3), the S pattern had only a single Midlatitude Westerlies (MW) region poleward of the subtropical anticyclone axis. The new conceptual model (Fig. 4) includes both a M/PF and a M/MW pattern/region to distinguish between cases that may move southeastward considerable distances before turning eastward in the midlatitude westerlies. Thus, a large number of M/PF tracks (Fig. 22) exist in both the South Indian and South Pacific Oceans. Some

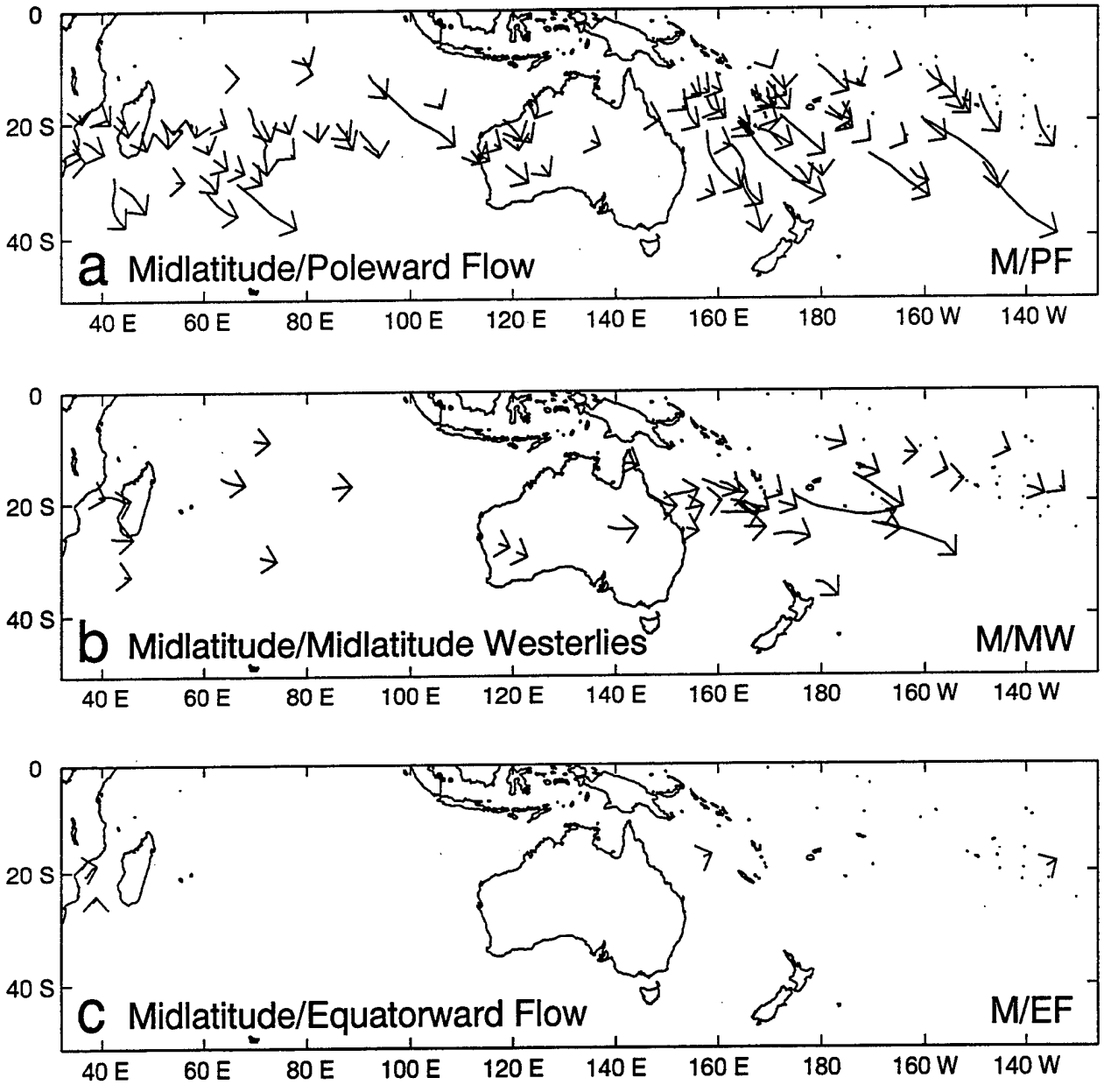

Fig. 22. Tracks as in Fig. 19, except in the Midlatitude (M) pattern and Poleward Flow (PF), Midlatitude Westerlies (MW), and Equatorward Flow (EF) regions.

of these tracks are quite long, and many of those extending far poleward had previously been classified as being in the P/PO pattern/region by Bannister *et al.* (1998; their Fig. 6).

Most of the tracks in the M/MW pattern/region are only short segments (Fig. 22), especially for the few (1.3%) cases in the South Indian Ocean. Evidently, the vertical wind shear in the Southern Hemisphere midlatitude westerlies is so strong that the TC is not sustained very long. The few longer M/MW tracks in the South Pacific (overall 8.9% of all cases) are at relatively low latitudes (~ 20-25° S) and may be cases with smaller vertical wind shear.

The new M/Equatorward Flow (EF) pattern/region is very rarely observed with only 0.4% (0.3%) in the South Indian (Pacific) Ocean (Fig. 18). Only two TCs in each basin experienced this unusual steering flow, and those tracks are very short (Fig. 22). The forecaster needs to be aware that such anomalous equatorward steering flow exists on the southeastern flank of the subtropical anticyclone.

b. *Environmental structure transitions*

Since each synoptic pattern/region in Fig. 4 has a characteristic track direction and speed as in Figs. 19 - 22, the transition from one pattern/region to another will be accompanied by a track change. Thus, it is important for the forecaster to anticipate that such a transition will occur during the forecast interval. Transitional mechanisms that can lead to a change in environment structure are listed in Fig. 2. Many case studies with synoptic analyses and tracks associated with the more important transitions are given in Bannister *et al.* (1997, 1998).

The purpose of this section is to update the transition frequency summary given in Bannister *et al.* (1998) based on the new synoptic pattern/region definitions and including also the 1998-1999 season. With the 14 observed synoptic pattern/region combinations for the Southern Hemisphere, many transitions are theoretically possible. Since many of the transitions have

occurred three or fewer times in the nearly nine full season sample, only the "recurring" (i.e., four or more cases) transitions are included in Fig. 23. Among the 161 TCs that spent all or part of their existence in the South Indian Ocean (Fig. 23a) during the period, 394 recurring transitions occurred, which is an average of about five transitions in environment structure for every two TCs. Among the 103 TCs that spent all or part of their existence in the South Pacific Ocean (Fig. 23b) during the period, 187 recurring transitions occurred, which is an average of about two transitions in environment structure per TC.

The complex appearance of these transition diagrams highlights the fact that many different transition paths are possible. These many possible transitions are particularly evident in the South Indian Ocean, especially for the Standard/Tropical Easterlies (S/TE) pattern/region, which is the most common environment structure. Clearly, this S/TE pattern/region is the "center of action" for transitions from and to various environment structures. However, remember that the only transition paths that are of concern to the forecaster at any time are those that are leaving the particular pattern/region combination that characterizes the present environment of the TC. Analyses of the relative frequency, and thus the climatological probability, of each transition path are in the following diagrams for the 14 synoptic pattern/region combinations.

1. Transitions from the Standard (S) pattern. The panels in Fig. 24 show the relative probabilities for transitions from the four synoptic regions of the S Pattern in the South Indian Ocean (upper four) and South Pacific Ocean (lower four). These percentages are based on all transitions from the specific pattern/region within the circle, and thus may differ from the numbers along the arrows in Fig. 23, which omit those transitions that occurred less than four times during the 1990-91 through 1998-99 seasons. To simplify some of the diagrams, a few

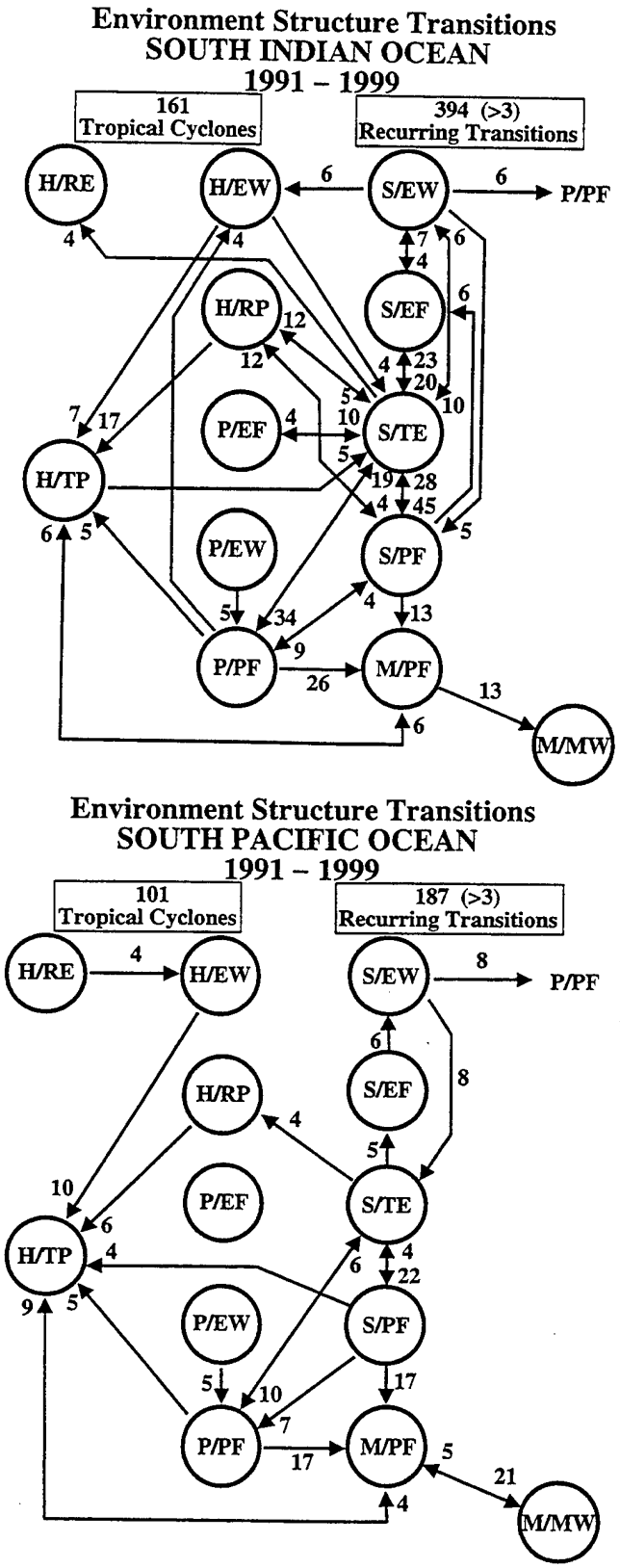

Fig. 23. Recurring (greater than three) environment structure transitions for the (a) 161 TCs in the South Indian Ocean and (b) 101 TCs in the South Pacific Ocean during the 1990-1991 through 1998-1999 seasons.

transitions that occurred only once are omitted here, and the percent of cases omitted is indicated in the lower right hand box. Notice that for some of the synoptic regions certain transition paths are much more likely than others, and these are denoted by broader arrows. A listing of these more probable transition paths from the S pattern/regions and the possible transition mechanisms is given in Table 1.

Consider the transitions from the S/TE pattern/region in the South Indian Ocean (Fig. 24, upper right), which is the most active environment structure in Fig. 23a. Recall that a TC in the S/TE pattern/region will be moving westward on the equatorward side of the subtropical anticyclone. The two most common environment transitions (34% and 26%) are to the Poleward Flow (PF) regions of either the S or the Poleward (P) patterns, respectively. With the addition of the 9% transitions to the High-amplitude (H)/Ridge Poleward (RP) pattern/region, 69% of all transitions are to an environmental steering with a more poleward component. The candidate transitional mechanisms for the most frequent S/TE to S/PF transition are listed in Table 1 as Advection (ADV), Beta-effect Propagation (BEP), Midlatitude CycloGenesis (MCG), and Semi-direct Cyclone Interaction on the Eastern TC (SCIE). Whereas the first two transitional mechanisms would be a simple translation around the subtropical anticyclone circulation, the third and fourth mechanisms involve a midlatitude cyclogenesis on the poleward side or another cyclone (usually a TC) to the west. By contrast, three recurring transitions from the S/TE pattern/region are indicated in Fig. 24 (top right) that lead to an equatorward steering flow, but only the S/EF frequently occurs (18% versus 3% for P/EF or H/RE). As indicated in Table 1, the candidate S/TE to S/EF transitional mechanisms are Midlatitude AnticycloGenesis (MAG) or SCI on the western TC (SCIW), which are again remote effects on either the poleward side or

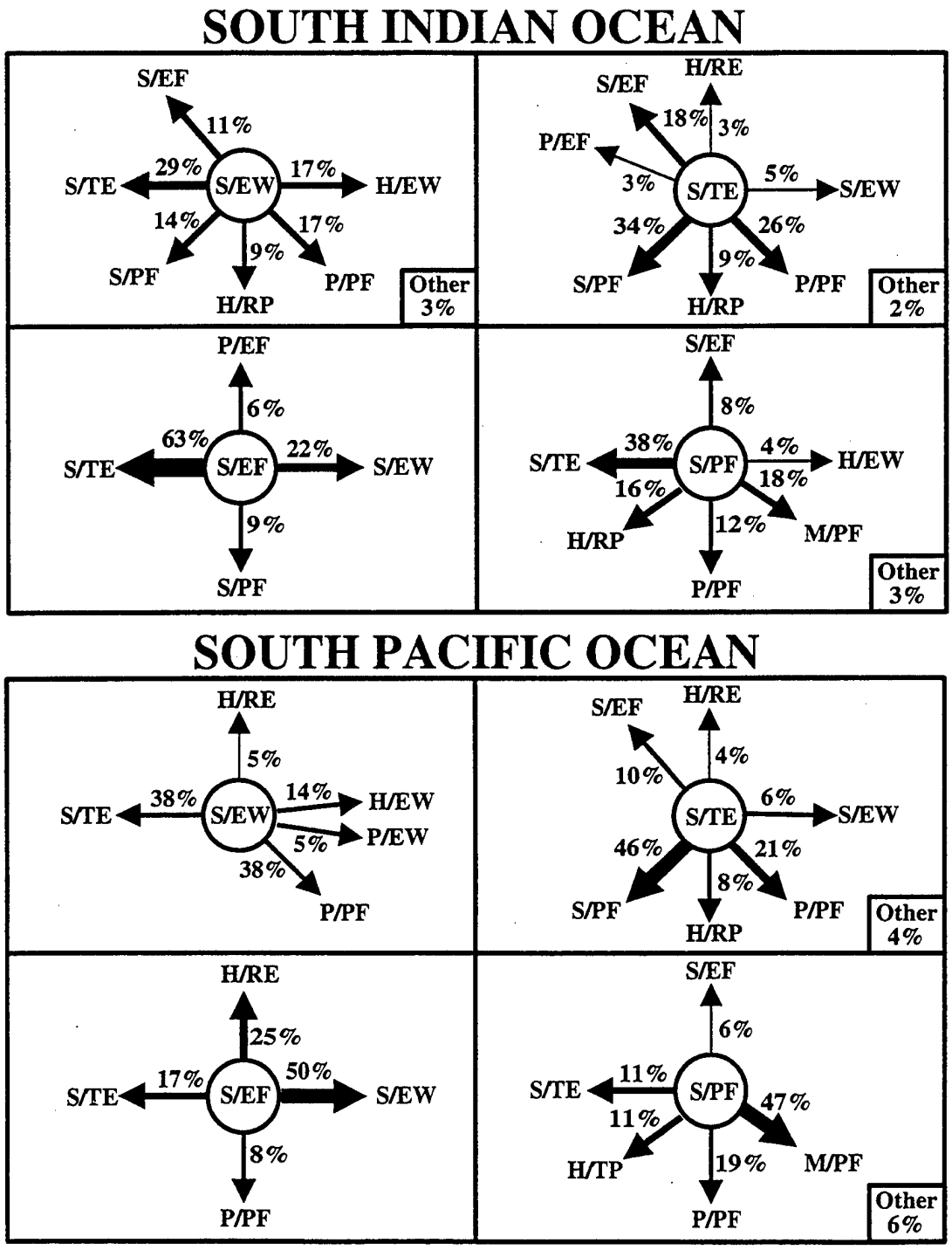

Figure 24. Percentages of transitions from the four synoptic regions of the Standard (S) pattern for TCs in the South Indian (top) and Pacific (bottom) Oceans during 1990-1991 through 1998-1999 seasons. A few transitions that occurred only once during the period are omitted, and the percent of these omitted transitions is indicated in the lower right in each box. More frequent transitions are represented by broader arrows.

from a cyclone (usually a TC) to the east. Finally, a reversal from a westward steering flow in S/TE to an eastward steering flow in the S/EW pattern/region is quite rare (5%).

Table 1. Summary of the more frequent transition paths from the Standard (S) synoptic regions as shown in Fig. 24 for either the South Pacific (SP) or South Indian Ocean (SIO), or both basins (column 2). Various candidate transitional mechanisms (see acronym definitions in the lower half of Fig. 2) are listed in the right column. An asterisk indicates that the transitional mechanism requires the presence of another cyclone (usually a TC or precursor/remnant) at the proper distance and orientation from the subject TC.

Transitions	Basin(s)	Candidate transitional mechanism(s)
S/EW to S/TE	Both	ADV, MAG, or MCL
S/EW to P/PF	SP	RMT, or RTF*
S/TE to S/PF	Both	ADV, BEP, MCG, or SCIE*
S/TE to P/PF	Both	RMT, or RTF*
S/TE to S/EF	SIO	MAG, or SCIW*
S/EF to S/TE	SIO	ADV, or MAL
S/EF to S/EW	SP	EWB
S/PF to S/TE	SIO	MAG, or MCL
S/PF to M/PF	SP	ADV, BEP, MCG
S/PF to P/PF	SWP	RMT, or RTF*

The transitions from the S/TE pattern/region in the South Pacific Ocean (Fig. 24) are somewhat simpler with 75% (14%) of the transitions leading to a poleward (equatorward) steering component. Here, the dominant transition mechanism is S/TE to S/PF with 46% of all transitions.

Consider also the possible transitions for an eastward-moving TC in the S/Equatorial Westerlies (S/EW) pattern/region in the South Indian Ocean (Fig. 24, upper left). Although slightly more (29%) of the transitions are to a westward steering in the S/TE pattern/region, 40% (sum of 14%, 9%, and 17% in the S/PF, H/RP, and P/PF combinations) of the transitions lead directly to a poleward steering flow. As listed in Table 1, the S/EW to S/TE transitional mechanisms are ADV, MAG, or Midlatitude CycloLysis (MCL), and the S/EW to P/PF

transitional mechanisms are Ridge Modification by a TC (RMT) or Reverse-oriented monsoon Trough Formation (RTF), which both involve a peripheral anticyclone building to the northeast. Other transition possibilities from S/EW in the South Indian Ocean are for a continued eastward steering in a H/EW pattern/region under the influence of a deeply penetrating midlatitude trough, or an equatorward (and westward) steering flow in the S/EF pattern/region.

Again, a more limited set of likely transitions from the S/EW pattern/region is found in the South Pacific compared to the South Indian Ocean. Two dominant transitions (38% each) are for a westward steering flow in S/TE or a poleward steering flow in the P/PF pattern/region. The only other transition from S/EW in the South Pacific with greater than 10% frequency is for a continued eastward steering in the H/EW pattern/region under the influence of a deeply penetrating midlatitude trough.

A TC in the S/Equatorward Flow (S/EF) pattern/region is relatively rare and generally persists for only a short period (Fig. 19). Keeping in mind that the statistics may be uncertain with these small sample sizes, an interesting contrast is found between the predominant transitions from the S/EF pattern/region in the South Indian and South Pacific Oceans (Fig. 24). Whereas 63% (22%) of the transitions from S/EF are to the S/TE (S/EW) pattern/region in the South Indian Ocean, a nearly opposite pattern is found with 17% (50%) in the South Pacific. As listed in Table 1, the candidate transitional mechanisms for S/EF to S/TE are ADV and Midlatitude AnticycloLysis (MAL), whereas the S/EF to S/EW transition in the South Pacific is likely to be due to an Equatorial Westerly wind Burst (EWB) as described by Bannister *et al.* (1998). Since the subsequent track following these transitions from S/TE is westward (eastward), these differences between the two ocean basins could be quite significant.

A TC in the S/PF pattern/region is moving poleward toward the subtropical ridge axis, and thus is approaching recurvature. The transition frequencies from S/PF in Fig. 24 indicate the possibilities. Surprisingly, the most frequent (38%) transition from S/PF in the South Indian Ocean is to return to a westward steering flow in the S/TE pattern/region, which leads to a "stairstep track" of westward, poleward, and then westward. The candidate S/PF to S/TE transitional mechanisms are MAG (or MCL) as the subtropical anticyclone becomes re-established poleward of the TC (Table 1). Three transitions from S/PF to another poleward steering flow are also possible (Fig. 24). In the case of the transitions to the H/RP (16%) or the P/PF (12%) pattern/region, the dominant steering flow circulation switches from the subtropical anticyclone to a high-amplitude midlatitude anticyclone or peripheral anticyclone, respectively. However, the TC is still equatorward of the subtropical ridge axis. The S/PF to P/PF transitional mechanism is either RMT or RTF (Table 1). Only 18% of the transitions from the S/PF pattern/region in the South Indian Ocean are directly to the Midlatitude (M)/PF pattern/region in which advection around the subtropical anticyclone leads to the typical recurvature track in other basins. These frequencies of transitions from the S/PF pattern/region indicate the transient nature of the TC environment in the South Indian Ocean, which makes forecasting difficult.

The transitions from the S/PF pattern/region in the South Pacific Ocean are more limited and straight-forward than in the South Indian Ocean (Fig. 24). Notice especially the dominant (47%) transitions to the M/PF pattern/regions, which is the typical recurvature track. In combination with the transitions to the H/Trough Poleward (TP) or the P/PF pattern/region that also have poleward steering flows, a South Pacific TC in the S/PF pattern/region has a 77% likelihood of continuing poleward, versus an 11% (6%) likelihood of changing to a westward (equatorward) steering flow.

Although the transition summaries in Fig. 23 appear to be very complicated, the TC at any time is only in one pattern/region and the forecaster only needs to be concerned with possible transitions from that pattern/region. The transition frequencies as in Fig. 24 narrow the possibilities. Given the more likely transitions, the forecaster can associate these with the transitional mechanisms from Table 1, which then indicates what adjacent circulations or physical processes the forecaster should determine either exist or do not exist. If a transitional mechanism results in a TC environment structure change, a corresponding track change should be expected. If none of the transitional mechanisms are present, it is expected that the TC will continue in the same pattern/region with a persistent track.

2. Transitions from the Poleward (P) pattern. The relative probabilities for transitions from the three synoptic regions of the P pattern in the South Indian Ocean and South Pacific Ocean are shown in Fig. 25. These percentages are based on all transitions from the specific pattern/region within the upper and lower panels in the circle, and thus may differ from the numbers along the arrows in Fig. 23, which omit those transitions that occurred less than four times during the 1990-91 through 1998-99 seasons. As in Fig. 24, a few transitions that occurred only once are omitted, and the percent of cases omitted is indicated in the lower-right box.

Some of the P pattern synoptic regions have certain transition paths that are much more likely than others. Even though the transitions from P/EW and P/EF are infrequent (see Fig. 23), it is significant that 100% of them were to P/PF and S/TE, respectively, for this sample. The candidate transitional mechanisms for the P/EW to P/PF transition are ADV, RMT, and RTF (Table 2). In the latter two transitions, a peripheral anticyclone building to the northeast will lead to a poleward steering flow. The likely P/EF to S/TE transitional mechanism is related to the dissipation or recurvature of the western TC and its associated peripheral anticyclone that had

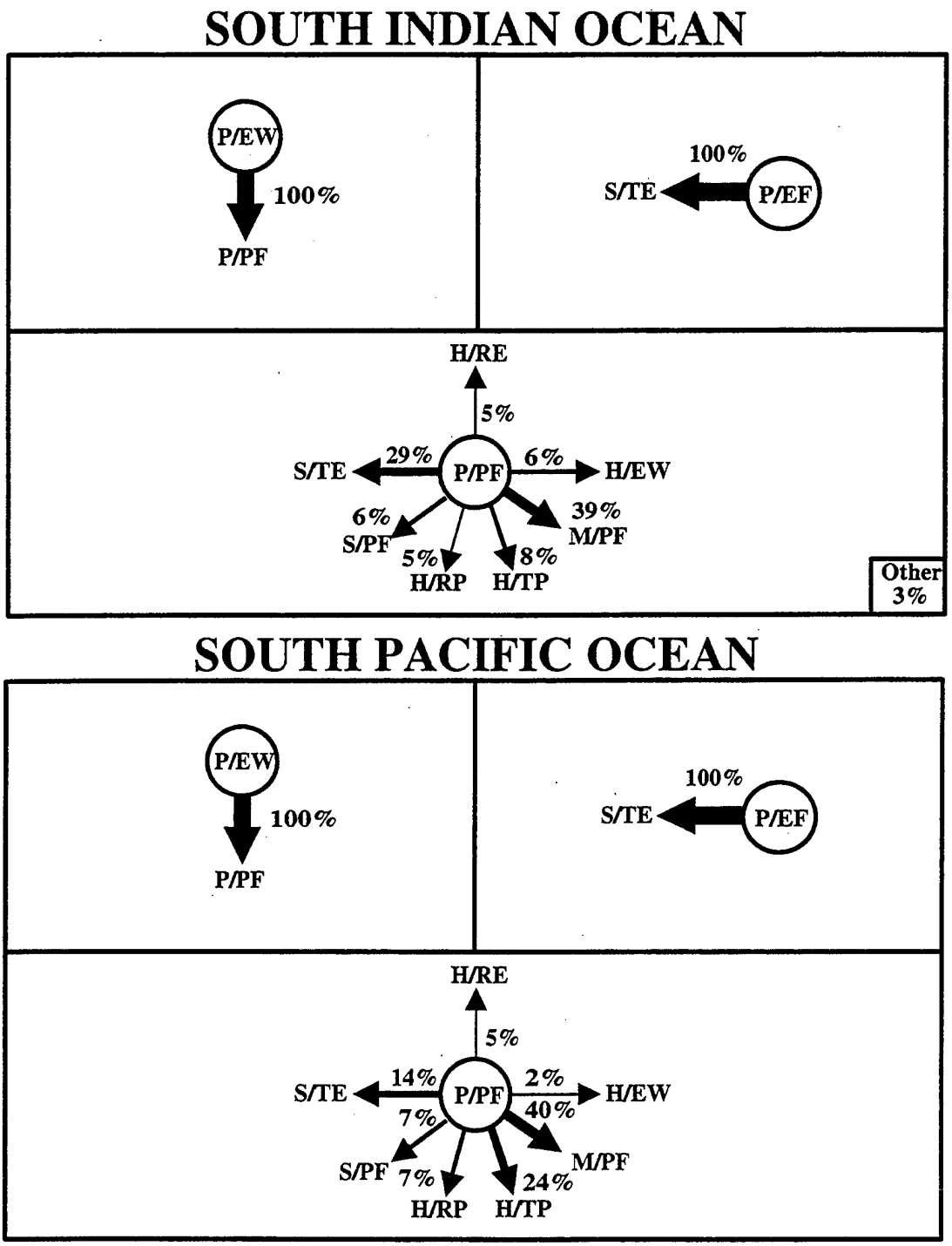

Fig. 25. Percentages of transitions from various synoptic regions as in Fig. 24, except for the Poleward (P) pattern.

Table 2. Transitional mechanisms as in Table 1, except for the more frequent transition paths from the P pattern synoptic regions as in Fig. 25.

Transitions	Basin(s)	Candidate transitional mechanism(s)
P/EW to P/PF	Both	ADV, RMT, RTF*
P/EF to S/TE	Both	Dissipation/recurvature of western TC
P/PF to M/PF	Both	ADV
P/PF to S/TE	SIO	MAG

originally established the EF region and determined the motion of the target storm.

The primary transition from the P/PF pattern/region in both oceans is to the M/PF pattern/region with about 40% of all transitions (Fig. 25). This transition would be due to advection through the subtropical anticyclone axis into the midlatitude westerlies. Whereas South Indian Ocean TCs in the P/PF pattern/region may turn westward following the 29% transitions to the S/TE pattern/region, only 14% of the South Pacific transitions would lead to a similar turn. The transitional mechanism in these cases is MAG as the subtropical anticyclone builds poleward of the TC (Table 2). The only other transitions from the P/PF pattern/region with greater than 10% in either basin is the 24% to the H/TP pattern/region in the South Pacific Ocean, which occurs when a high-amplitude trough becomes the more dominant steering mechanism.

3. Transitions from the High-amplitude (H) pattern. Following the pattern established above, the relative probabilities are calculated for transitions from the four synoptic regions of the H Pattern in the South Indian Ocean (Fig. 26, upper) and South Pacific Ocean (Fig. 26, lower). Since the occurrence of TCs in the H/Ridge Equatorward (H/RE) is rare, the transition frequencies from that pattern/region are subject to change. One new aspect from this study is the H/RE to H/EW transition, which accounted for 44% of the H/RE transitions in the

South Pacific Ocean. The most frequent H/RE transition in the South Indian Ocean is to the S/TE pattern/region with a westward steering flow equatorward of the subtropical anticyclone. The transitional mechanism in both of these cases is simply advection.

Perhaps the most significant finding for the transitions from the H/RP pattern/region in both oceans (Fig. 26) is that they nearly always are to another poleward flow environment, and especially the H/TP pattern/region via the MCG transitional mechanism as the high-amplitude trough becomes the dominant steering flow (Table 3). In the South Pacific Ocean, only two other poleward flow transitions (12% each to S/PF and M/PF) occurred. In the South Indian Ocean, 14% and 7% of the transitions are to the S/PF and M/PF pattern/regions, respectively. A significant fraction (17%) of the transitions from the H/RP pattern/region in the South Indian Ocean are to the S/TE pattern/region, so that the poleward-moving TC would turn westward.

Table 3. Transitional mechanisms as in Table 1, except for the more frequent transition paths from the H pattern synoptic regions as in Fig. 26.

Transitions	Basin(s)	Candidate transitional mechanism(s)
H/RP to H/TP	Both	MCG
H/EW to H/TP	Both	ADV, MCG
H/TP to M/PF	SP	ADV

Another relatively infrequent H pattern/region is the H/EW. These preliminary statistics (Fig. 26) would indicate the dominant transition from H/EW is to the H/TP pattern/region, especially in the South Pacific with 56% of these transitions. Another option is to continue eastward in a S/EW pattern/region with 17% of the transitions in both oceans, or to turn westward in a S/TE pattern/region with 22% (11%) of the transitions in the South Indian (Pacific) Ocean. It is also possible that a poleward turn in the P/PF pattern/region (17% in the South Pacific Ocean) or an equatorward turn in the H/RE pattern/region (17% in the South

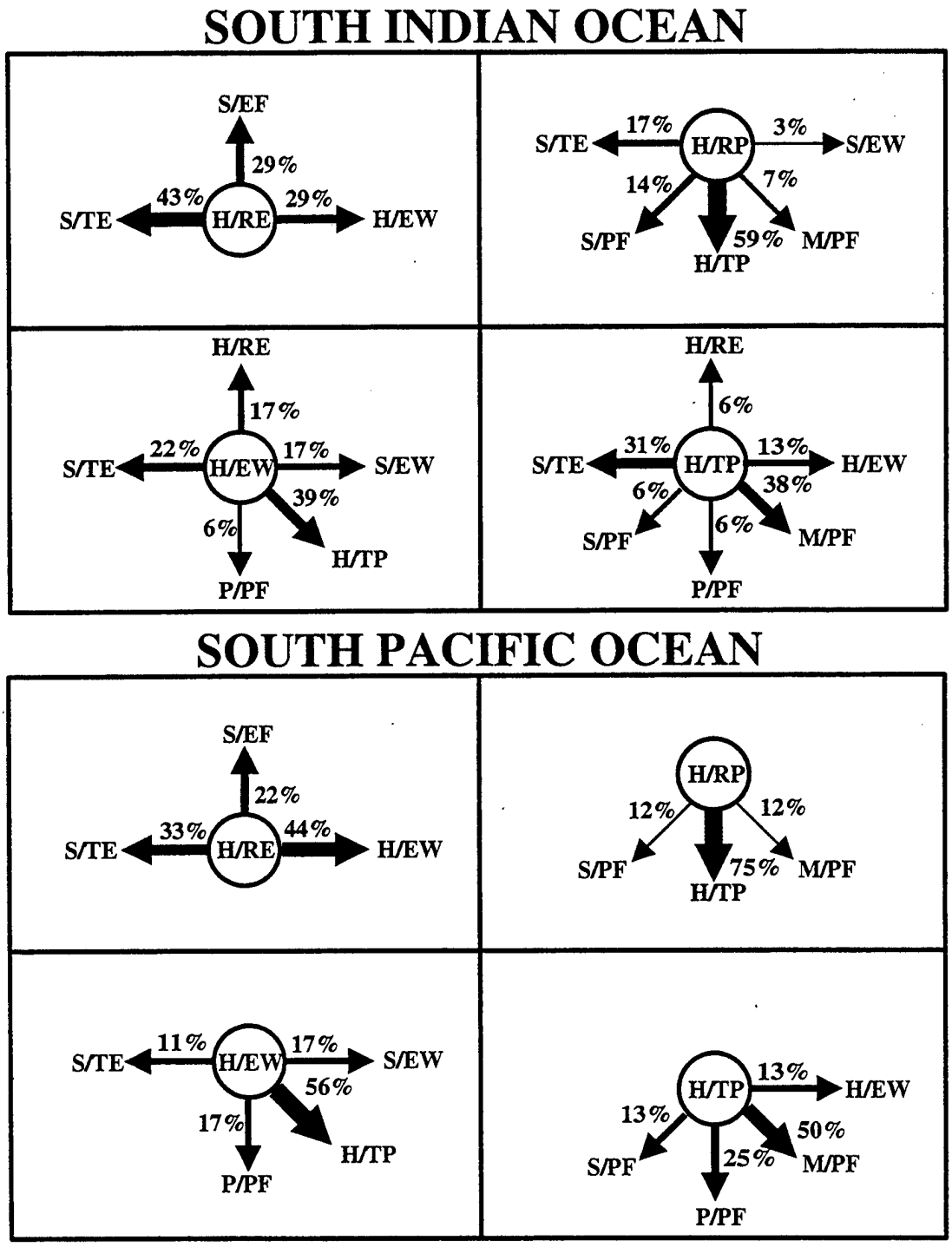

Fig. 26. Percentages of transitions from various synoptic regions as in Fig. 24, except for the High-amplitude (H) pattern.

Indian Ocean) will follow a transition from eastward motion in the H/EW pattern/region. Thus, this situation of a TC in a H/EW pattern/region may be considered rather uncertain.

The most common H pattern/region is the H/TP, which has a poleward (and often strong) steering flow east of a deeply penetrating midlatitude trough. The most favored transition from H/TP is to the M/PF pattern/region with 50% (38%) of the cases in the South Pacific (Indian Ocean), which means that the TC is advected through the subtropical anticyclone axis into the midlatitude westerlies (Table 3). Other options for continued poleward flow for a TC in the South Pacific are transitions to the P/PF (25%) or to the S/PF (13%) pattern/region. By contrast, these transitions only account for 6% each of the South Indian transitions from H/TP. A highly frequent transition from H/TP in the South Indian Ocean is to the S/TE pattern/region, as the subtropical anticyclone becomes re-established via the MAG transitional mechanism and the poleward-moving TC will then turn westward. Surprisingly, 13% of the transitions from H/TP in both oceans were to the H/EW pattern/region, which would indicate an eastward steering flow. This transition can occur if the midlatitude trough weakens or passes eastward such that the TC is at the equatorward end of the trough.

4. Transitions from the Midlatitude (M) pattern. As for the previous three patterns, the relative probabilities are calculated for transitions from the three synoptic regions of the M pattern in the South Indian Ocean (Fig. 27, upper) and South Pacific Ocean (Fig. 27, lower).The most common pattern/region is the M/PF, which is just poleward of the subtropical anticyclone axis. Both in the South Indian and Pacific Oceans, the dominant transition from the M/PF pattern/region is to the M/Midlatitude Westerlies (M/MW) pattern/region, with 50% and 60% of the transitions, respectively. The transitional mechanism (Table 4) is simply advection around the poleward side of the subtropical anticyclone. The only other frequent transition from the

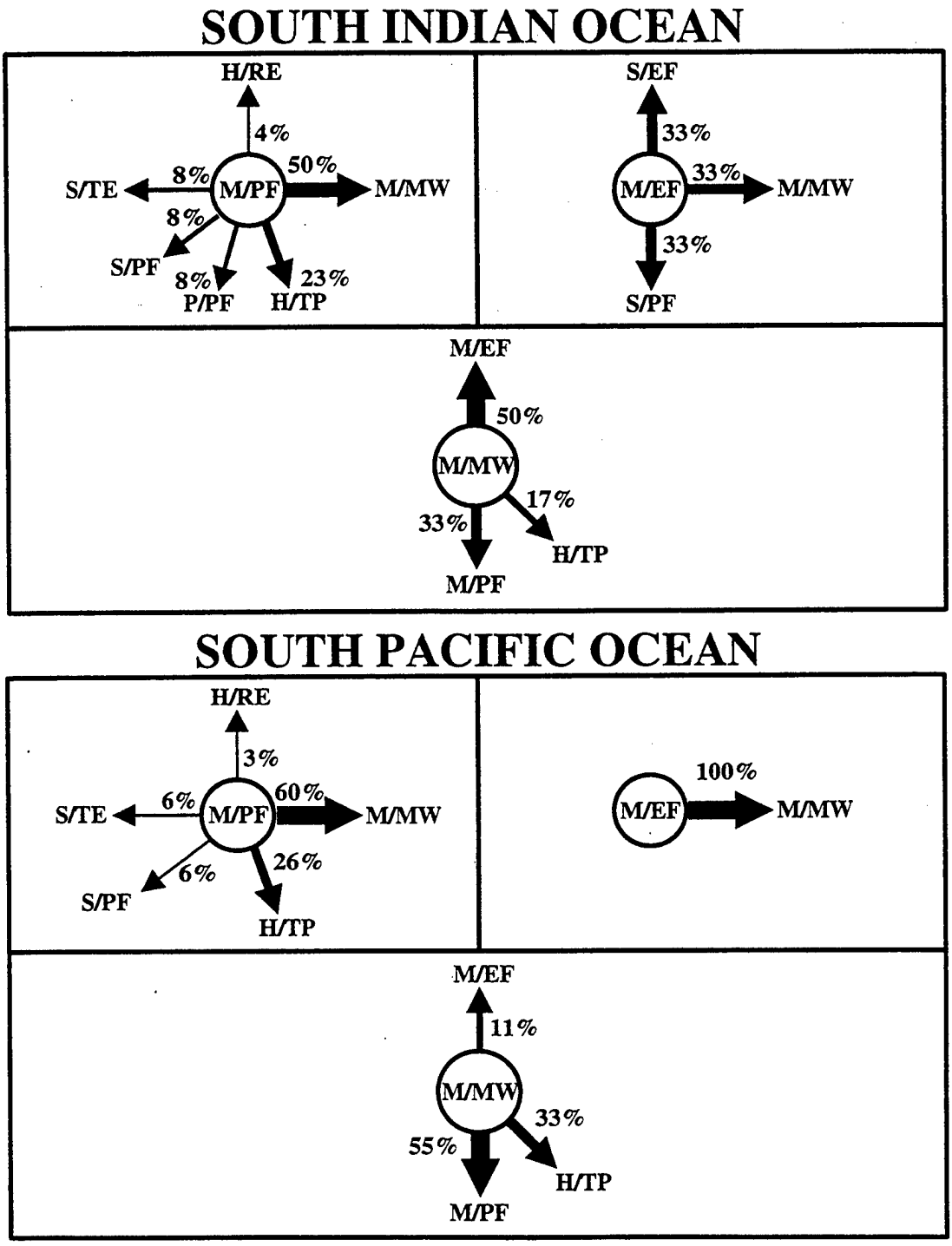

Fig. 27. Percentages of transitions from various synoptic regions as in Fig. 24, except for the Midlatitude (M) pattern.

M/PF pattern/region is to the H/TP pattern/region, which accounts for 23% (26%) of the transitions in the South Indian (Pacific) Oceans. In this transition, an approaching high-amplitude trough becomes the dominant steering flow, which is the MCG transitional mechanism (Table 4).

Transitions from the M/Equatorward Flow (EF) pattern/region occurred less than four times in both oceans and thus do not appear in Fig. 23. Even though the transitions from M/EF are shown in Fig. 27 for completeness, the percentages are not reliable and will not be discussed. A Midlatitude AnticycloLysis (MAL) would account for the M/EF to M/MW transition (Table 4).

Although Southern Hemisphere TCs in the M/MW pattern/region typically dissipate, those transitions from this pattern/region are summarized in Fig. 27. Keeping in mind the small samples, half of the transitions for South Indian TCs in the M/MW pattern/region are to the M/EF pattern/region, while only 11% of the South Pacific transitions from M/MW pattern/region were to the equatorward flow region. For the South Pacific Ocean, the predominant (55%) transition from the M/MW is to the M/PF pattern/region. An alternate transition is to the H/TP pattern/region, and in both cases MCG would be the transitional mechanism. The corresponding transition frequencies are 33% and 17% for the South Indian Ocean.

Table 4. Transitional mechanisms as in Table 1, except for the more frequent transition paths from the M pattern as in Fig. 27.

Transitions	Basin(s)	Candidate transitional mechanism(s)
M/PF to M/MW	Both	ADV
M/PF to H/TP	Both	MCG
M/EF to M/MW	SP	MAL
M/MW to M/EF	SIO	MAG, ADV
M/MW to M/PF	SP	MCG

4. Summary and conclusions

The Meteorological knowledge base of the Systematic Approach to tropical cyclone track forecasting in the Southern Hemisphere has been updated, as defined in Fig. 4. In the new terminology, the synoptic regions are labeled with a directionality of the TC steering flow. New definitions include a Midlatitude (M) synoptic pattern whenever the TC is poleward of the subtropical anticyclone axis, and this pattern has four synoptic regions. Other new pattern/region combinations are Equatorward Flow regions in the Standard (S) and Poleward (P) patterns, and a P/Equatorial Westerlies (EW) pattern/region. Examples of these new environment structures in operational (NOGAPS) analyses and tracks are given in section 2. Perhaps the most important conclusion is that all cases in the 1990-91 through 1998-1999 seasons could be classified into one of these 14 synoptic pattern/region combinations. The nine-year "climatology" of the occurrences of each of the 14 combinations is given in Fig. 18 for the South Indian and Pacific Oceans separately. The characteristic tracks in each of these 14 combinations are shown in Figs. 19-22.

In addition to new synoptic pattern/region combinations that have been defined, some new transitional mechanisms between these combinations have been defined (Fig. 2, bottom). For example, the Midlatitude System Evolution conceptual model in Fig. 8 includes four transitional mechanisms: Midlatitude CycloGenesis (MCG), CycloLysis (MCL), AnticycloGenesis (MAG), and AnticycloLysis (MAL). The importance of these transitions from one pattern/region combination to another is that the TC track then also changes as indicated in Figs. 19-22. The frequency of recurring (greater than three) transitions in this nine-year sample is summarized in Fig. 23. Because the TC is at any time in only one pattern/region combination, the concern of the forecaster is on the possible transitions <u>from</u> that pattern/region. To assist the

forecaster, the percentages of these transitions from each pattern/region combination are summarized in Figs. 24-27. Some of these transitions are clearly more favored than others, which is useful guidance to the forecaster.

This updated and refined Meteorological knowledge base should be useful to the Southern Hemisphere TC forecaster. First, the revised Systematic Approach conceptual models of the synoptic pattern/regions appear useful for describing the present motion of the TC. Recognition of the transitional mechanisms described here is critical to forecasting future TC track changes, which is the goal for the Systematic Approach.

Future research will examine the capability of dynamical models to forecast Southern Hemisphere TC tracks following the approach of Carr and Elsberry (1999), who define eight conceptual models for frequently occurring error mechanisms. Each of these error mechanisms arises when the dynamical model incorrectly predicts the TC-environment structure and/or structure changes, and thus are incorrect predictions of the transitional mechanisms in Fig. 2. If these error mechanisms conceptual models also apply in the Southern Hemisphere, this will provide a tool to assist the forecaster in deciding which dynamical model track forecasts should be used as guidance for the official track forecast.

REFERENCES

Bannister, A. J., M. A. Boothe, L. E. Carr, III, and R. L. Elsberry, 1997: Southern Hemisphere application of the systematic approach to tropical cyclone track forecasting. Part I. Environmental structure characteristics. Tech. Rep. NPS-MR-98-001, Naval Postgraduate School, Monterey, CA 93943-5114, 96 pp.

Bannister, A. J., M. A. Boothe, L. E. Carr, III, and R. L. Elsberry, 1998: Southern Hemisphere application of the systematic approach to tropical cyclone track forecasting Part II. Climatology and refinement of Meteorological knowledge base. Tech. Rep. NPS-MR-98-004, Naval Postgraduate School, Monterey, CA 93943-5114, 69 pp.

Boothe, M. A., 1997: Extension of the systematic approach to tropical cyclone track forecasting in the eastern and central Pacific. Master's Thesis, Naval Postgraduate School, Monterey, CA 93943, 133 pp.

Boothe, M. A., R. L. Elsberry, and L. E. Carr, III, 1999: Atlantic application of the Systematic Approach to tropical cyclone track forecasting. Part I: Environmental structure characteristics. Tech. Rep. NPS-MR-99-003, Naval Postgraduate School, Monterey, CA 93943-5114, in press.

Carr, L. E., III, and R. L. Elsberry, 1994: Systematic and integrated approach to tropical cyclone track forecasting. Part I. Approach overview and description of meteorological basis. Tech. Rep. NPS-MR-94-002, Naval Postgraduate School, Monterey, CA 93943-5114, 273 pp.

Carr, L. E., III, and R. L. Elsberry, 1997: Models of tropical cyclone wind distribution and beta-effect propagation for application to tropical cyclone track forecasting. *Mon. Wea. Rev.*, **125**, 3190-3209.

Carr, L. E., III, and R. L. Elsberry, 1999: Systematic and integrated approach to tropical cyclone track forecasting. Part III: Traits knowledge base for JTWC track forecast models in the western North Pacific. Tech. Rep. NPS-MR-99-002, Naval Postgraduate School, Monterey, CA 93943-5114, 227 pp.

Carr, L. E., III, M. A. Boothe, S. R. White, C. S. Kent, and R. L. Elsberry, 1995: Systematic and integrated approach to tropical cyclone track forecasting. Part II. Climatology, reproducibility, and refinement of meteorological data base. Tech. Rep. NPS-MR-95-001, Naval Postgraduate School, Monterey, CA 93943-51143, 96 pp.

Carr, L. E., III, M. A. Boothe, and R. L. Elsberry, 1997: Observational evidence for alternate modes of track-altering binary tropical cyclone scenarios. *Mon. Wea. Rev.*, **125**, 2094-2111.

Kent, C. S. T., 1995: Systematic and integrated approach to tropical cyclone track forecasting in the North Atlantic. Master's Thesis, Naval Postgraduate School, Monterey, CA 93943, 76 pp.

White, S. R., 1995: Systematic and integrated approach to tropical cyclone track forecasting in the eastern and central North Pacific. Master's Thesis, Naval Postgraduate School, Monterey, CA 93943, 79 pp.

DISTRIBUTION LIST

Space and Naval Warfare Systems Command PWM 185 4301 Pacific Highway San Diego, CA 92110-3127	4
Dr. Carlyle H. Wash, Chairman Department of Meteorology, MR/Wx Naval Postgraduate School 589 Dyer Rd., Room 254 Monterey, CA 93943-5114	1
Dr. Russell L. Elsberry Department of Meteorology, MR/Es Naval Postgraduate School 589 Dyer Rd., Room 254 Monterey, CA 93943-5114	80
Library, Code 0142 Naval Postgraduate School Monterey, CA 93943	2
Dean of Research, Code 09 Naval Postgraduate School Monterey, CA 93943	1
Defense Technical Information Center Cameron Station Alexandria, VA 22304-6145	2